

TECHNICAL RESEARCH REPORT

Feedback Control of Border Collision Bifurcations in Two-Dimensional Discrete-Time Systems

*by Munther A. Hassouneh, Eyad H. Abed,
Soumitro Banerjee*

TR 2002-36



ISR develops, applies and teaches advanced methodologies of design and analysis to solve complex, hierarchical, heterogeneous and dynamic problems of engineering technology and systems for industry and government.

ISR is a permanent institute of the University of Maryland, within the Glenn L. Martin Institute of Technology/A. James Clark School of Engineering. It is a National Science Foundation Engineering Research Center.

Web site <http://www.isr.umd.edu>

Feedback Control of Border Collision Bifurcations in Two-Dimensional Discrete-Time Systems

Munther A. Hassouneh[†], Eyad H. Abed[†] and Soumitro Banerjee[‡]

[†]Department of Electrical and Computer Engineering
and the Institute for Systems Research

University of Maryland, College Park, MD 20742 USA

abed@eng.umd.edu

[‡]Department of Electrical Engineering

Indian Institute of Technology, Kharagpur 721302, India

31 August 2002

Abstract

The feedback control of border collision bifurcations is considered for two-dimensional discrete-time systems. These are bifurcations that can occur when a fixed point of a piecewise smooth system crosses the border between two regions of smooth operation. The goal of the control effort is to modify the bifurcation so that the bifurcated steady state is locally unique and locally attracting. In this way, the system's local behavior is ensured to remain stable and close to the original operating condition. This is in the same spirit as local bifurcation control results for smooth systems, although the presence of a border complicates the bifurcation picture considerably. Indeed, a full classification of border collision bifurcations isn't available, so this paper focuses on the more desirable (from a dynamical behavior viewpoint) cases for which the theory is complete. The needed results from the analysis of border collision bifurcations are succinctly summarized. The control design is found to lead to systems of linear inequalities. Any feedback gains that satisfy these inequalities is then guaranteed to solve the bifurcation control problem. The results are applied to an example to illustrate the ideas.

1 Introduction

The purpose of this paper is to study the feedback control of border collision bifurcations in two-dimensional piecewise smooth maps. Similar control problems have been considered for one-dimensional systems by the authors in [1, 2]. The study of border collision bifurcations in two-dimensional systems is significantly more complicated than for one-dimensional systems. Indeed, a full classification of border collision bifurcations is not yet available. Thus, we focus on designing feedback control laws that can be shown to ensure that the system

undergoing a border collision bifurcation will experience a safe (locally stable) form of such bifurcations. To achieve this, we collect analysis results from the literature on these more desirable bifurcations, giving details only on those for which clear and proven sufficient conditions exist. The control laws considered allow for actuation on either side of a border of a piecewise smooth system, or on both sides, or on both sides with the restriction that the same control gains apply on both sides of the border.

Continuous piecewise-smooth dynamical systems have been found to undergo special bifurcations along the borders between regions of smooth dynamics. These have been named border collision bifurcations by Nusse and Yorke [3], and had been studied in the Russian literature under the name C-bifurcations by Feigin [4]. Di Bernardo et al. [5] brought Feigin's results in a more complete form to a wider audience while putting them in the context of modern bifurcation analysis. Border collision bifurcations include bifurcations that are reminiscent of the classical bifurcations in smooth systems such as fold and period doubling bifurcations.

Despite this resemblance, the classification of border collision bifurcations (BCB) is far from complete, and certainly very preliminary in comparison to the results available in the smooth case. The classification is complete only for one-dimensional discrete-time systems [6, 7]. Concerning the two-dimensional piecewise smooth maps, Banerjee and Grebogi [8] propose a classification for a class of two-dimensional maps undergoing border-collision by exploiting a normal form. It has also recently been shown by Banerjee, Yorke and Grebogi [9] that the dynamics of two-dimensional piecewise-smooth (PWS) maps may feature so-called robust chaotic dynamics without parameter windows of periodic behavior. Dutta et al. [10] presented a novel analysis showing that in border collision bifurcation in which multiple coexisting attractors are created simultaneously cause the intriguing phenomenon that in the presence of arbitrarily small noise the bifurcations lead to fundamentally unpredictable behavior of orbits as a system parameter is varied slowly through its bifurcation value. Di Bernardo et al. [11] analyzed a so-called corner-collision bifurcation (which is a border-collision bifurcation) in piecewise-smooth systems of ordinary differential equations. For higher dimensional systems, currently the known results are limited to several rather general observations.

Since the discovery of border collision bifurcations, several researchers have studied bifurcations in PWS systems [3, 12, 13, 14, 15, 8, 7, 16, 5, 17, 18]. PWS systems occur as models for switched systems, such as power electronic circuits (e.g., [15]) and impacting mechanical systems (e.g., [19, 20, 21, 22, 17, 18]). They are usually modeled by piecewise smooth maps. PWS discrete-time maps are also used to model systems that are inherently discrete. For example, it has been recently shown that simple computer networks with Transmission Control Protocol (TCP) connections and implementing a Random Early Detection (RED) algorithm at the router end can be modeled as PWS maps [23]. Other examples of PWS discrete time systems which have been shown to exhibit BCBs can be found in economics (e.g., [24]), biology (e.g., [25]) and in controlled linear discrete time systems with PWS nonlinearity (e.g., [26]). PWS systems can of course exhibit classical smooth bifurcations, for example at a fixed point in a neighborhood of which the system is smooth. What is of interest therefore is the study of bifurcations in PWS systems that occur at the boundaries between regions of smooth behavior, or that involve motions that include more than one such region.

In this paper, the goal is to obtain feedback control laws to ensure a less severe form of

border collision bifurcation than could otherwise occur. Since a full classification of possible border collision bifurcations isn't available, it is crucial that sufficient conditions that are known for the desirable border collision bifurcations be summarized clearly.

It should be emphasized that, while this paper focuses on maps, the results have implications for switched continuous-time systems as well. Maps provide a concise representation that facilitates the investigation of system behavior and control design. They are also the natural models for many applications, as mentioned above. Even for a continuous piecewise smooth system, a control design derived using the map representation can be translated to a continuous controller either analytically or numerically.

The only studies we know of on control of BCBs are Di Bernardo [27], Di Bernardo and Chen [28] and our work [1, 2]. In [27, 28], feedbacks functioning only on the unstable side of the border were sought to modify the bifurcation from one type to another type using the classification scheme of Feigin. The control gains were chosen by trial and error. In [1, 2], we considered design of feedbacks that achieve safe BCBs for one-dimensional discrete-time systems. This could entail feedback on either side of the border or on both sides. Sufficient conditions for stabilizing control gains were found analytically.

This paper is organized as follows. In Section 2, we summarize sufficient conditions for safe border collision bifurcation in two dimensional maps. In Section 3, we develop feedback control laws to modify the border collision bifurcation to one that is less severe. In Section 4, the results are applied to an example model system that has been used in studies of cardiac nodal conduction time.

2 Sufficient Conditions for Safe Border Collision Bifurcations in Two-Dimensional Systems

In this section, we summarize the known sufficient conditions for the simplest safe border collision bifurcations, i.e., for border collision bifurcations that involve a locally stable fixed point leading to a locally unique stable fixed point or a locally unique stable period-two orbit after the border. More precisely, we summarize only those cases for which it has been proven that the bifurcated fixed point or period-two orbit is part of a locally unique bifurcated family of orbits. That is, no other periodic or chaotic steady state orbits emerge in the cases we discuss. We focus on these simple supercritical cases since in the control design part of the paper, our goal will be to find control laws that render the system's operation to satisfy one of the sufficient conditions.

2.1 General classification

The investigations into border collision bifurcations phenomena were initiated by mathematicians looking into the dynamics of piecewise smooth (PWS) maps [4, 3]. Later the development benefited from the observation that most power electronic circuits yield piecewise smooth maps under discrete-time modeling, and nonsmooth bifurcations are quite common in them [15].

In a two-dimensional PWS map, the stability of the fixed points is determined by the

eigenvalues or, equivalently, by the trace and the determinant of the corresponding Jacobian matrices. There have been two approaches in developing a classification of the border collision bifurcations. The work of the Russian mathematician Feigin [4] (which was brought to the English-speaking world in [5]) considered the existence of period-1 and period-2 orbits before and after border collision, and classified the various cases depending on the number of real eigenvalues greater than 1 or less than -1 . This resulted in a powerful strategy of giving a general classification of border-collision bifurcations in n -dimensional piecewise smooth systems. However, this general classification of BCBs does not provide detailed classification of various border collision bifurcations which is needed in developing stabilizing feedback control laws.

Other authors tried to tackle this problem with reference to one- and two-dimensional maps by using other techniques of nonlinear dynamics. For example [16, 8] looked at the asymptotically stable orbits (including chaotic orbits) before and after border collision, and proved the existence of various types of BCBs, depending on the relationship of the trace and the determinant of the Jacobian matrix on the two sides of the border.

Consider a PWS map that involves only two regions of smooth behavior:

$$f(x, y, \mu) = \begin{cases} f_A(x, y, \mu), & (x, y) \in R_A \\ f_B(x, y, \mu), & (x, y) \in R_B \end{cases} \quad (1)$$

where μ is the bifurcation parameter and R_A and R_B are regions of smooth behavior. Since the system is two-dimensional, the border is a curve separating the two regions of smooth behavior and is given by $x = h(y, \mu)$. The map $f : \mathfrak{R}^2 \times \mathfrak{R} \rightarrow \mathfrak{R}^2$ is assumed to be PWS: f depends smoothly on (x, y) everywhere except at the border where it is continuous in (x, y) . It is also assumed that f depends smoothly on μ everywhere, and the Jacobian elements are finite at both sides of the border.

Let $(x_0(\mu), y_0(\mu))$ be a possible path of fixed points of f ; this path depends continuously on μ . Suppose also that the fixed point hits the border at a critical parameter value μ_b .

Since the nature of border collision bifurcations depends on the local character of the map in the neighborhood of the fixed point, it suffices to look at the piecewise linear approximation at the two sides of the border. It has been shown that a *normal form* for the PWS system (1) in the neighborhood of a fixed point on the border can be expressed as [3, 8, 16]

$$\begin{aligned} \begin{pmatrix} x_{k+1} \\ y_{k+1} \end{pmatrix} &= G_2(x_k, y_k, \mu) \\ &= \begin{cases} \underbrace{\begin{pmatrix} \tau_L & 1 \\ -\delta_L & 0 \end{pmatrix}}_{\mathbf{J}_L} \begin{pmatrix} x_k \\ y_k \end{pmatrix} + \begin{pmatrix} 1 \\ 0 \end{pmatrix} \mu, & x_k \leq 0 \\ \underbrace{\begin{pmatrix} \tau_R & 1 \\ -\delta_R & 0 \end{pmatrix}}_{\mathbf{J}_R} \begin{pmatrix} x_k \\ y_k \end{pmatrix} + \begin{pmatrix} 1 \\ 0 \end{pmatrix} \mu, & x_k \geq 0 \end{cases} \quad (2) \end{aligned}$$

where τ_L is the trace and δ_L is the determinant of the Jacobian matrix \mathbf{J}_L of the system at a fixed point in $R_A := \{(x, y) \in \mathfrak{R}^2 : x \leq 0\}$ and close to the border and τ_R is the trace and δ_R is the determinant of the Jacobian matrix \mathbf{J}_R of the system evaluated at a fixed point in

$R_B := \{(x, y) \in \mathfrak{R}^2 : x \geq 0\}$ near the border. The normal form map $G_2(\cdot, \cdot, \cdot)$ can be used to study local bifurcations of the original PWS map [8, 16] when a fixed point collides with the border.

Denote by $L^* := (x_L^*, y_L^*) \in R_A$ and $R^* := (x_R^*, y_R^*) \in R_B$ possible fixed points of the system near the border. Then from the normal form (2), the fixed points are given by:

$$(x_L^*, y_L^*) = \left(\frac{\mu}{1 - \tau_L + \delta_L}, \frac{-\mu\delta_L}{1 - \tau_L + \delta_L} \right), \quad (3)$$

$$(x_R^*, y_R^*) = \left(\frac{\mu}{1 - \tau_R + \delta_R}, \frac{-\mu\delta_R}{1 - \tau_R + \delta_R} \right). \quad (4)$$

For the fixed point L^* to actually occur, one needs $\frac{\mu}{1 - \tau_L + \delta_L} \leq 0$, otherwise L^* is in R_B and is denoted as \bar{L}^* , a virtual fixed point. Similarly, for R^* to actually occur, one needs $\frac{\mu}{1 - \tau_R + \delta_R} \geq 0$. Otherwise, R^* is in R_A and is denoted as \bar{R}^* . The stability of the fixed points is determined by the eigenvalues of the corresponding Jacobian matrix

$$\lambda_{1,2} = \frac{1}{2} \left(\tau \pm \sqrt{\tau^2 - 4\delta} \right)$$

The results on BCBs in two-dimensional systems available in the literature require that $|\delta_L| < 1$ and $|\delta_R| < 1$ ¹. Therefore, in the control design phase of this work we will need to ensure that the closed-loop system satisfies this condition (along with other conditions to be presented below).

There can be six types of fixed points in a linearized dissipative two-dimensional discrete system when the determinant is positive (Table 1). The fixed points in two sides of a border collision may be any of these six types.

The following result is very useful.

Proposition 1 *When the eigenvalues at both sides of the border are real, if an attracting orbit exists, it is unique (i.e., coexisting attractors cannot occur).*

Proof:

(a) If the fixed points in both sides are saddles, the attractor can be a period-2 or chaos, both of which occur on the unstable manifolds of the saddles. Now, The stable eigenvector at R^* has a positive slope $m_1 = (-\delta_R/\lambda_{1R})$, and the unstable eigenvector at L^* has a negative slope given by $(-\delta_L/\lambda_{1L})$. Therefore a heteroclinic intersection must exist. There is a mathematical result, called the Lambda Lemma [30], which says that if a curve C crosses a stable manifold transversely, then each point of the unstable manifold of the same saddle fixed point is a limit point of $\bigcup_{n>0} f^n(C)$. Since the unstable manifold of L^* has transverse intersections with the stable manifold of R^* , by the Lambda Lemma we conclude that the two unstable manifolds come arbitrarily close to each other. Therefore the attractor must be unique.

¹It has been shown that attractors can exist if the determinant in one side is greater than unity in magnitude, provided that determinant in the other side is smaller than unity. The situation $|\delta_L| > 1$ and $\delta_R = 0$ (which occurs in some classes in power electronic systems) has been treated in [29].

Table 1: The possible types of fixed points of the normal form map.

Type	eigenvalues	condition
For positive determinant		
Regular attractor	real, $0 < \lambda_1, \lambda_2 < 1$	$2\sqrt{\delta} < \tau < (1 + \delta)$
Regular saddle	real, $0 < \lambda_1 < 1, \lambda_2 > 1$	$\tau > (1 + \delta)$
Flip attractor	real, $-1 < \lambda_1 < 0, -1 < \lambda_2 < 0$	$-(1 + \delta) < \tau < -2\sqrt{\delta}$
Flip saddle	real, $-1 < \lambda_1 < 0, \lambda_2 < -1$	$\tau < -(1 + \delta)$
Spiral attractor	complex, $ \lambda_1 , \lambda_2 < 1$	
(a) Clockwise spiral		$0 < \tau < 2\sqrt{\delta}$
(b) Counter-clockwise spiral		$-2\sqrt{\delta} < \tau < 0$
For negative determinant		
Flip attractor	$-1 < \lambda_1 < 0, 0 < \lambda_2 < 1$	$-(1 + \delta) < \tau < (1 + \delta)$
Flip saddle	$\lambda_1 > 1, -1 < \lambda_2 < 0$	$\tau > 1 + \delta$
Flip saddle	$0 < \lambda_1 < 1, \lambda_2 < -1$	$\tau < -(1 + \delta)$

(b) If the fixed points in both sides are stable and eigenvalues are real, for $\mu < 0$ initial conditions in R_A converge on the stable manifold associated with the larger eigenvalue, and then converge on to L^* along that eigenvector. All initial conditions in R_B see the virtual fixed point \bar{R}^* which is in R_A , and move to R_A along a stable manifold. Now, it has been shown in [16] that this stable manifold folds at the intersection with the x -axis, and this ensures the existence of a transverse heteroclinic intersection with a stable manifold of L^* . This implies that the stable manifolds of L^* and \bar{R}^* come arbitrarily close to each other, and therefore all initial conditions in R_B also converge on to L^* . The same argument applies for $\mu > 0$, and trajectories starting from all initial conditions converge on the stable fixed point L^* .

(c) If the fixed point in R_A is stable and that in R_B is unstable, then for $\mu < 0$ a mechanism like case (b) operates and for $\mu > 0$ a mechanism like case (a) operates, preventing the occurrence of coexisting attractors. ■

Next, we summarize the known cases in which a locally unique fixed point before the border yields, after the border, either a new locally unique fixed point or a locally unique period-2 attractor. The discussion begins with the case in which the system determinants are positive on both sides of the border, followed by the case in which the determinants are negative on both sides of the border, ending with the cases in which the determinants on both sides of the border are of opposite signs.

2.2 The case of positive determinants on both sides of the border

Scenario A. Locally unique stable fixed point on both sides of the border

If

$$-(1 + \delta_L) < \tau_L < (1 + \delta_L) \quad \text{and} \quad -(1 + \delta_R) < \tau_R < (1 + \delta_R) \quad (5)$$

then a stable fixed point persists as the bifurcation parameter μ is increased (or decreased)

through zero. The possible changes in the type of fixed point for the positive determinants case, and the resultant system behavior are summarized in Table 2. These border collision events can happen either with or without extraneous periodic orbits emerging from the critical point. This table summarizes the present knowledge about the possibility of extraneous bifurcated orbits (EBO) occurring either before, after, or on both sides of the border for the various cases. “Possible” means examples exist where EBOs occur at bifurcation. “Possible*” means that we know of no such examples, but also no proof has been reported that EBOs do not occur. The cases where EBOs are known not to occur (i.e., the fixed points on both sides of the border are locally unique and stable) are those in which the eigenvalues are real both before and after the border (see Proposition 1). This happens when the fixed point changes from: 1) regular attractor to flip attractor 2) regular attractor to regular attractor 3) flip attractor to regular attractor and 4) flip attractor to flip attractor, as μ is varied through its critical value (see cases 1-4 in Table 2).

Scenario B. Supercritical period doubling BCB

When the determinants on both sides of the border are positive, there are two regions in the parameter space where period doubling BCB occurs (a locally unique stable fixed point leads to an unstable fixed point plus a locally unique attracting period two orbit). These scenarios of interest in this paper result from either of two sets of conditions, and is therefore divided into Scenario B1 and Scenario B2 as follows.

Scenario B1. This occurs if

$$-(1 + \delta_L) < \tau_L < -2\sqrt{\delta_L}, \quad (6)$$

$$\tau_R < -(1 + \delta_R), \quad (7)$$

$$\text{and} \quad \tau_R \tau_L < (1 + \delta_R)(1 + \delta_L). \quad (8)$$

Scenario B2. This occurs if

$$2\sqrt{\delta_L} < \tau_L < (1 + \delta_L), \quad (9)$$

$$\tau_R < -(1 + \delta_R), \quad (10)$$

$$\text{and} \quad \tau_R \tau_L > -(1 - \delta_R)(1 - \delta_L). \quad (11)$$

2.3 The case of negative determinants on both sides of the border

If the determinants on both sides of the border are negative, then the eigenvalues are real. Thus if the fixed point is stable, it is locally unique (see Proposition 1). The condition for locally unique stable fixed point on both sides of the border is given in Scenario C below.

Scenario C. Locally unique stable fixed point on both sides of the border

If the determinants on both sides of the border are negative, a locally unique stable fixed point leads to a locally unique stable fixed point as μ is increased through zero if

$$-(1 + \delta_L) < \tau_L < (1 + \delta_L) \quad \text{and} \quad -(1 + \delta_R) < \tau_R < (1 + \delta_R). \quad (12)$$

Table 2: For the parameter range given by (5) (the positive determinants case), a stable fixed point yields a stable fixed point after the border crossing. However, this can happen either with or without extraneous periodic orbits (EBO) emerging from the critical point. “Possible” means examples exist where EBOs occur at bifurcation. “Possible*” means that we know of no such examples, but also no proof has been reported that EBOs do not occur.

Case no.	Type of fixed points	Parameter space region	Possibility of EBOs
1	Regular attractor to flip attractor	$2\sqrt{\delta_L} < \tau_L < (1 + \delta_L),$ $-(1 + \delta_R) < \tau_R < -2\sqrt{\delta_R}$	Not Possible
2	Regular attractor to Regular attractor	$2\sqrt{\delta_L} < \tau_L < (1 + \delta_L),$ $2\sqrt{\delta_R} < \tau_R < (1 + \delta_R)$	Not Possible
3	Flip attractor to Regular attractor	$-(1 + \delta_L) < \tau_L < -2\sqrt{\delta_L},$ $2\sqrt{\delta_R} < \tau_R < (1 + \delta_R)$	Not Possible
4	Flip attractor to Flip attractor	$-(1 + \delta_L) < \tau_L < -2\sqrt{\delta_L},$ $-(1 + \delta_R) < \tau_R < -2\sqrt{\delta_R}$	Not Possible
5	Regular attractor to spiral attractor	$2\sqrt{\delta_L} < \tau_L < (1 + \delta_L),$ $-2\sqrt{\delta_R} < \tau_R < 2\sqrt{\delta_R}$	Possible*
6	Spiral attractor to Regular attractor	$-2\sqrt{\delta_L} < \tau_L < 2\sqrt{\delta_L},$ $2\sqrt{\delta_R} < \tau_R < (1 + \delta_R),$	Possible*
7	Flip attractor to Spiral attractor	$-(1 + \delta_L) < \tau_L < -2\sqrt{\delta_L},$ $-2\sqrt{\delta_R} < \tau_R < 2\sqrt{\delta_R}$	Possible
8	Spiral attractor to Flip attractor	$-2\sqrt{\delta_L} < \tau_L < 2\sqrt{\delta_L},$ $-(1 + \delta_R) < \tau_R < -2\sqrt{\delta_R}$	Possible
9	Clockwise spiral to Anticlockwise spiral	$0 < \tau_L < 2\sqrt{\delta_L},$ $-2\sqrt{\delta_R} < \tau_R < 0$	Possible
10	Anticlockwise spiral to Clockwise spiral	$-2\sqrt{\delta_L} < \tau_L < 0,$ $0 < \tau_R < 2\sqrt{\delta_R}$	Possible
11	Clockwise spiral to Clockwise spiral	$0 < \tau_L < 2\sqrt{\delta_L},$ $0 < \tau_R < 2\sqrt{\delta_R}$	Possible*
12	Anticlockwise spiral to Anticlockwise spiral	$-2\sqrt{\delta_L} < \tau_L < 0,$ $-2\sqrt{\delta_R} < \tau_R < 0$	Possible*

Also, the condition for supercritical period doubling border collision with no EBOs is:

Scenario D: Supercritical border collision period doubling

If

$$-(1 + \delta_L) < \tau_L < (1 + \delta_L), \quad (13)$$

$$\tau_R < -(1 + \delta_R), \quad (14)$$

$$\tau_R \tau_L < (1 + \delta_R)(1 + \delta_L), \quad (15)$$

$$\text{and} \quad \tau_R \tau_L > -(1 - \delta_R)(1 - \delta_L). \quad (16)$$

then a locally unique stable fixed point to the left of the border for $\mu < 0$ crosses the border and becomes unstable and a locally unique period two orbit is born as μ is increased through zero.

2.4 The case of negative determinant to the left of the border and positive determinant to the right of the border

If the determinant is negative to the left of the border, then the eigenvalues are real. If the determinant is positive to the right of the border, then the eigenvalues are real if $\tau_R^2 > 4\delta_R$. Thus, a sufficient condition for having a locally unique fixed point leading to a locally unique fixed point as μ is varied through the critical value is given as:

Scenario E. Locally unique stable fixed point on both sides of the border

$$-(1 + \delta_L) < \tau_L < (1 + \delta_L), \quad (17)$$

$$-(1 + \delta_R) < \tau_R < (1 + \delta_R), \quad (18)$$

$$\text{and} \quad \tau_R^2 > 4\delta_R \quad (19)$$

The conditions can be divided into two cases:

Scenario E1. This occurs if

$$-(1 + \delta_L) < \tau_L < (1 + \delta_L) \quad (20)$$

$$\text{and} \quad -(1 + \delta_R) < \tau_R < -2\sqrt{\delta_R} \quad (21)$$

Scenario E2. This occurs if

$$-(1 + \delta_L) < \tau_L < (1 + \delta_L) \quad (22)$$

$$\text{and} \quad 2\sqrt{\delta_R} < \tau_R < (1 + \delta_R) \quad (23)$$

2.5 The case of positive determinant to the left of the border and negative determinant to the right of the border

If the determinant is negative to the right of the border, then the eigenvalues are real. If the determinant is positive to the left of the border, then the eigenvalues are real if $\tau_L^2 > 4\delta_L$.

Thus, a sufficient condition for having a locally unique fixed point leading to a locally unique fixed point as μ is varied through the critical value is given as:

Scenario F. Locally unique stable fixed point on both sides of the border

$$-(1 + \delta_L) < \tau_L < (1 + \delta_L), \quad (24)$$

$$\tau_L^2 > 4\delta_L, \quad (25)$$

and $-(1 + \delta_R) < \tau_R < (1 + \delta_R). \quad (26)$

The conditions can be divided into two cases:

Scenario F1. This occurs if

$$-(1 + \delta_L) < \tau_L < -2\sqrt{\delta_L} \quad (27)$$

and $-(1 + \delta_R) < \tau_R < (1 + \delta_R) \quad (28)$

Scenario F2. This occurs if

$$2\sqrt{\delta_L} < \tau_L < (1 + \delta_L) \quad (29)$$

and $-(1 + \delta_R) < \tau_R < (1 + \delta_R) \quad (30)$

Note that currently there are no known conditions for supercritical border collision period doubling that occurs without EBOs when the determinants on both sides of the border are of opposite signs.

Figures 1 and 2 is a compact representation of Scenarios A-F. They show the parameter ranges for τ_L , δ_L , τ_R and δ_R such that the fixed points are unique attractors on both sides of the border (in these figures, δ_L and δ_R are fixed whereas τ_L and τ_R are variables).

2.6 Undesirable and dangerous bifurcations

From the literature, we can also identify several bifurcations that lead to a collapse of the piecewise smooth system. Our interest here is in control to achieve safe (not dangerous) BCBs, but it is worthwhile summarizing some of the known conditions for dangerous BCBs. The “dangerous bifurcations” considered begin with a system operating at a stable fixed point on one side of the border, say the left side. The main “dangerous bifurcations” that can result from border collision are:

Border collision pair bifurcation: This occurs if

$$-(1 + \delta_L) < \tau_L < (1 + \delta_L)$$

and $\tau_R > (1 + \delta_R)$

where a stable fixed point and an unstable fixed point merge and disappear as μ is increased through zero. This is analogous to saddle node bifurcations in smooth maps. The system trajectory diverges for positive values of μ since no local attractors exist.

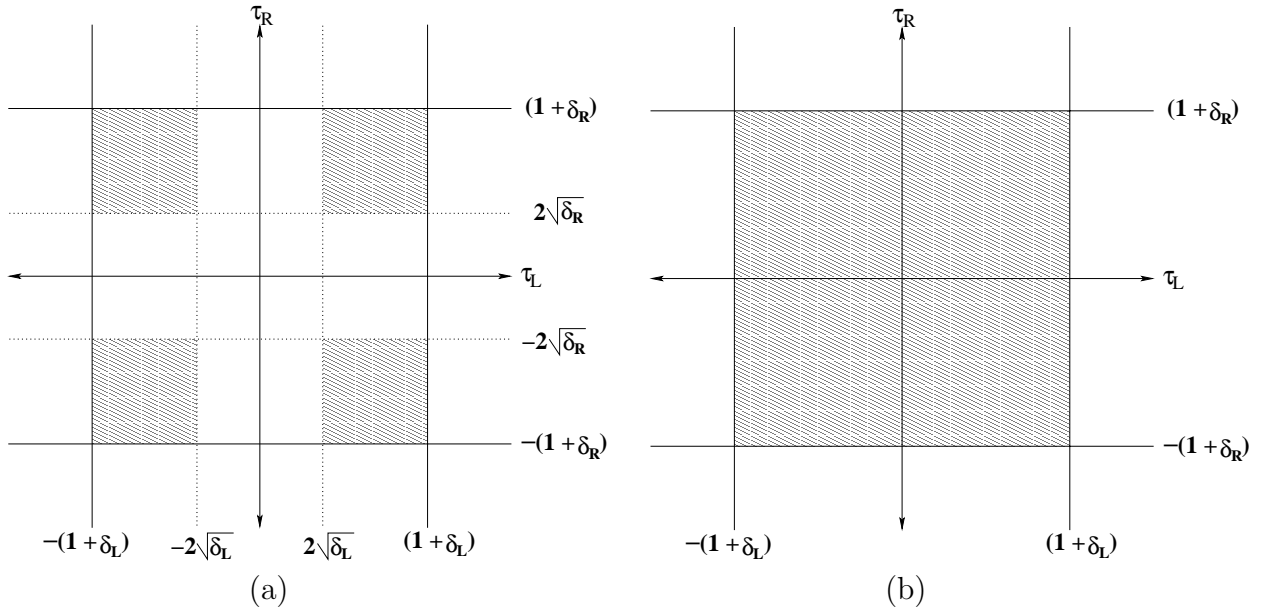


Figure 1: No bifurcation occurs as μ is increased (decreased) through zero in the shaded regions. Only the path of the fixed point changes at $\mu = 0$. (a) $0 < \delta_L < 1$ and $0 < \delta_R < 1$ (b) $-1 < \delta_L < 0$ and $-1 < \delta_R < 0$.

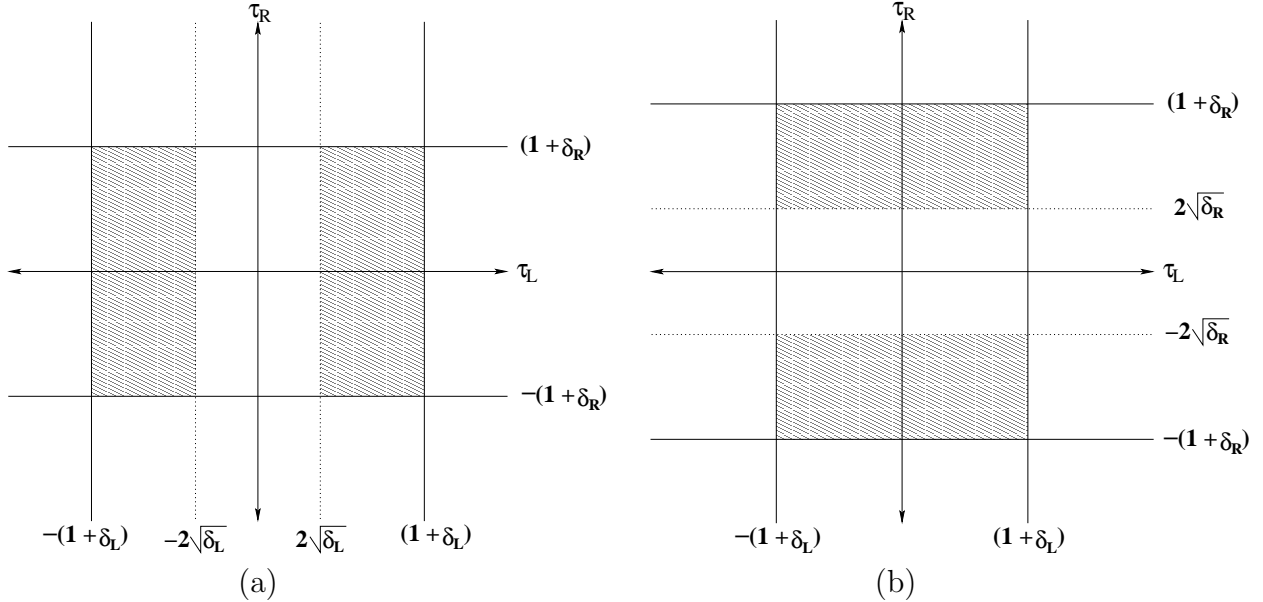


Figure 2: No bifurcation occurs as μ is increased (decreased) through zero in the shaded regions. Only the path of the fixed point changes at $\mu = 0$. (a) $0 < \delta_L < 1$ and $-1 < \delta_R < 0$ (b) $-1 < \delta_L < 0$ and $0 < \delta_R < 1$.

Subcritical border collision period doubling: This occurs if

$$\begin{aligned} -(1 + \delta_L) &< \tau_L < (1 + \delta_L), \\ \tau_R &< -(1 + \delta_R), \\ \text{and} \quad \tau_R \tau_L &> (1 + \delta_R)(1 + \delta_L). \end{aligned}$$

Here a bifurcation from a stable fixed point and an unstable period-2 orbit to the left of border to an unstable fixed point to the right of the border occurs as μ is increased through zero.

In addition, there are certain BCBs that, while not causing a catastrophic collapse of the system, may lead to undesirable system behavior. These include the following, conditions for which are given in [8, 16].

Stable fixed point leading to stable fixed point plus EBOs: This is an instance of multiple attractor bifurcation. In such a BCB, multiple attractors may occur on either side of the border or both sides of the border in addition to the stable fixed points. Conditions for this type of BCB are not currently available. Two examples of this are given in Section 3.

Supercritical border collision period doubling: Although supercritical period doubling is not classified as “dangerous bifurcation,” it is undesirable in some applications. (see Section 4 below for an example.)

Stable fixed point leading to chaos: This is also called instant chaos where chaotic behavior develops following border collision.

These are the situations that would require control. Next, we present the methodologies of controlling such undesirable and dangerous bifurcations.

3 Control of BCB in PWS Two-Dimensional Maps

In the remainder of the paper, control of BCBs in PWS maps of dimension two is discussed. The analysis leads to sufficient conditions on the control gains that are in the form of systems of linear inequalities. Software packages such as MATLAB have standard ways of checking for existence of solutions to such systems. Indeed, determining feasibility of constraints is a standard first step in solving linear programming problems.

Consider a general 2-D PWS map of the form

$$f(x, y, \mu) = \begin{cases} f_A(x, y, \mu), & (x, y) \in R_A \\ f_B(x, y, \mu), & (x, y) \in R_B \end{cases} \quad (31)$$

where μ is the bifurcation parameter and R_A, R_B are two regions of smooth behavior separated by a smooth curve called the border — $x = h(y, \mu)$. The map $f(\cdot, \cdot, \cdot)$ is assumed to be PWS: $f_A(x, y, \mu) := \begin{pmatrix} f_{A_1}(x, y, \mu) \\ f_{A_2}(x, y, \mu) \end{pmatrix}$ is smooth on R_A , $f_B(x, y, \mu) := \begin{pmatrix} f_{B_1}(x, y, \mu) \\ f_{B_2}(x, y, \mu) \end{pmatrix}$ is

smooth on R_B and f is continuous in (x, y) and depends smoothly on μ everywhere. Let $(x_0(\mu), y_0(\mu))$ be a possible path of fixed points of f ; this path depends continuously on μ . Suppose also that the fixed point hits the border at a critical parameter value μ_b . Assume without loss of generality that $\mu_b = 0$. Thus, $(x_0(0), y_0(0)) = (x_b, y_b)$. Suppose that the coordinate system is chosen such that $(x_b, y_b) = (0, 0)$.

Expanding (31) in a Taylor series near the fixed point $(0, 0, 0)$ gives

$$f(x, y, \mu) = \begin{cases} J_A \begin{pmatrix} x \\ y \end{pmatrix} + \begin{pmatrix} \alpha_1 \\ \alpha_2 \end{pmatrix} \mu + HOT, & (x, y) \in R_A \\ J_B \begin{pmatrix} x \\ y \end{pmatrix} + \begin{pmatrix} \alpha_1 \\ \alpha_2 \end{pmatrix} \mu + HOT, & (x, y) \in R_B \end{cases} \quad (32)$$

where J_A is the Jacobian of f at $(x, y) \in R_A$ close to $(0, 0, 0)$, J_B is the Jacobian of f at $(x, y) \in R_B$ close to $(0, 0, 0)$ and $\begin{pmatrix} \alpha_1 \\ \alpha_2 \end{pmatrix}$ is the derivative of f with respect to μ , and HOT denotes higher order terms. The quantities in (32) are thus:

$$J_A = \lim_{(x,y) \rightarrow (0^-, 0)} \begin{pmatrix} \frac{\partial f_{A_1}(x, y, 0)}{\partial x} & \frac{\partial f_{A_1}(x, y, 0)}{\partial y} \\ \frac{\partial f_{A_2}(x, y, 0)}{\partial x} & \frac{\partial f_{A_2}(x, y, 0)}{\partial y} \end{pmatrix}, \quad (33)$$

$$J_B = \lim_{(x,y) \rightarrow (0^+, 0)} \begin{pmatrix} \frac{\partial f_{B_1}(x, y, 0)}{\partial x} & \frac{\partial f_{B_1}(x, y, 0)}{\partial y} \\ \frac{\partial f_{B_2}(x, y, 0)}{\partial x} & \frac{\partial f_{B_2}(x, y, 0)}{\partial y} \end{pmatrix}, \quad (34)$$

and

$$\begin{pmatrix} \alpha_1 \\ \alpha_2 \end{pmatrix} = \lim_{(x,y) \rightarrow (0,0)} \begin{pmatrix} \frac{\partial f_{A_1}(x, y, 0)}{\partial \mu} \\ \frac{\partial f_{A_2}(x, y, 0)}{\partial \mu} \end{pmatrix} = \lim_{(x,y) \rightarrow (0,0)} \begin{pmatrix} \frac{\partial f_{B_1}(x, y, 0)}{\partial \mu} \\ \frac{\partial f_{B_2}(x, y, 0)}{\partial \mu} \end{pmatrix}. \quad (35)$$

Note that the limit in (35) is independent of the direction of approach to the origin since f is smooth in μ .

The fact that the normal form for BCBs contains only linear terms in the state leads one to seek linear feedback controllers to modify the system's bifurcation characteristics. The linear feedback can either be applied on only one side of the border or on both sides of the border. Both possibilities are considered below. The issue of which type of actuation to use and with what constraints is a delicate one. There are practical advantages to applying a feedback on only one side of the border, say the stable side. However, this requires knowledge of where the border lies, which is not necessarily available in practice. The purpose of pursuing stabilizing feedback acting on both sides of the border is to ensure robustness with respect to modeling uncertainty. This is done below by investigating the use of simultaneous stabilization as an option — that is, controls are sought that function in exactly the same way on both sides

of the border, while stabilizing the system's behavior. Not surprisingly, the conditions for existence of simultaneously stabilizing controls are more restrictive than for the existence of one sided controls.

The notion of applying different controls on the two sides of the border was previously considered by Bernardo [27]. This method provides some flexibility in controlling both sides of the border to any desirable behavior, but knowledge of the border is needed in the design. Here, the concept of applying the control to the stable side of the border only is also considered. This method will be shown to facilitate stabilization of the system to a period-2 orbit after the BCB in cases where the uncontrolled system bifurcates to an unstable fixed point or to a chaotic attractor.

All the control laws are developed based on the map linearizations as the fixed point is approached on both sides of the border. It is important to emphasize that we do not assume the system to be in normal form. This alleviates two problems: First, by not requiring the system to be in normal form, we need not include state transformations in the design of control laws except for the transformation setting the border to lie on the y -axis. Second, simultaneous control can be considered directly in a natural way. (Recall that in this paper simultaneous control occurs when we assume that a single feedback law applies on both sides of the border. If a normal form were used, then because two different linear transformations would be needed on both sides of the border to achieve the normal form, a simultaneous feedback in physical coordinates would not be simultaneous in normal form coordinates, and keeping track of the difference would be highly unwieldy.) Consider a general two-dimensional piecewise affine map

$$f(x, y, \mu) = \begin{cases} \underbrace{\begin{pmatrix} a_{11} & a_{12} \\ a_{13} & a_{14} \end{pmatrix}}_{\mathbf{J}_L} \begin{pmatrix} x \\ y \end{pmatrix} + \begin{pmatrix} \alpha_1 \\ \alpha_2 \end{pmatrix} \mu, & (x, y) \in R_L \\ \underbrace{\begin{pmatrix} a_{21} & a_{22} \\ a_{23} & a_{24} \end{pmatrix}}_{\mathbf{J}_R} \begin{pmatrix} x \\ y \end{pmatrix} + \begin{pmatrix} \alpha_1 \\ \alpha_2 \end{pmatrix} \mu, & (x, y) \in R_R \end{cases} \quad (36)$$

where μ is the bifurcation parameter and f is assumed continuous in \mathfrak{R}^2 but nonsmooth at the border separating R_L and R_R . Without loss of generality, let the border separating the two regions of smooth behavior be $x = 0$, i.e., $R_L = \{(x, y) \in \mathfrak{R}^2 : x \leq 0\}$ and $R_R = \{(x, y) \in \mathfrak{R}^2 : x > 0\}$. Since the map f is not differentiable at the border $x = 0$, $\mathbf{J}_L \neq \mathbf{J}_R$. The continuity of f at the border implies that the second column of \mathbf{J}_L equals the second column of \mathbf{J}_R , i.e., $a_{12} = a_{22} := a_2$ and $a_{14} = a_{24} := a_4$. Let $\tau_L := \text{trace}(\mathbf{J}_L) = a_{11} + a_4$, $\delta_L := \det(\mathbf{J}_L) = a_{11}a_4 - a_2a_{13}$, $\tau_R := \text{trace}(\mathbf{J}_R) = a_{21} + a_4$ and $\delta_R := \det(\mathbf{J}_R) = a_{21}a_4 - a_2a_{23}$.

Remark 1 *If the border is not $x = 0$ (without loss of generality, it can be assumed to pass through the origin), it can be transformed to $x = 0$ by introducing a shift in the x -variable: $\bar{x} = x - h(y, \mu)$ and leaving y unchanged: $\bar{y} = y$. Then in the (\bar{x}, \bar{y}) coordinates, $\bar{x} = 0$ is the border. It is assumed that this transformation has been done before the linearizations on both sides of the border were calculated (see [8]).*

Note that the map (36) in general represents the linearizations of a two-dimensional PWS map near a fixed point on the border separating two regions of smooth behavior R_L and R_R

as shown above. System (36) undergoes a variety of border collision bifurcations depending on the values of the parameters τ_L , δ_L , τ_R and δ_R as mentioned above. The fixed points of the map (36) on both sides of the border are given by

$$\begin{aligned} (x_L^*, y_L^*) &= \left(\frac{(\alpha_1 - \alpha_1 a_4 + a_2 \alpha_2) \mu}{1 - \tau_L + \delta_L}, \frac{(a_{13} \alpha_1 + \alpha_2 - \alpha_2 a_{11}) \mu}{1 - \tau_L + \delta_L} \right), \\ (x_R^*, y_R^*) &= \left(\frac{(\alpha_1 - \alpha_1 a_4 + a_2 \alpha_2) \mu}{1 - \tau_R + \delta_R}, \frac{(a_{23} \alpha_1 + \alpha_2 - \alpha_2 a_{21}) \mu}{1 - \tau_R + \delta_R} \right). \end{aligned}$$

Assume that $\alpha_1 - \alpha_1 a_4 + a_2 \alpha_2 \neq 0$ so that the fixed point does not move along the border as μ is varied through zero. Without loss of generality, assume $\alpha_1 - \alpha_1 a_4 + a_2 \alpha_2 > 0$ (if $\alpha_1 - \alpha_1 a_4 + a_2 \alpha_2 < 0$, just replace μ by $-\mu$).

Below, the Jury test for second order systems is recalled (see, for instance [31]) which will be used in the sequel. It gives necessary and sufficient conditions for Schur stability of characteristic polynomials of degree two.

Lemma 1 (Jury's Test for Second Order Systems [31]).

A necessary and sufficient condition for the zeros of the polynomial

$$p(\lambda) = \eta_2 \lambda^2 + \eta_1 \lambda + \eta_0 \tag{37}$$

($\eta_2 > 0$) to lie within the unit circle is

$$p(1) > 0, \quad p(-1) > 0 \quad \text{and} \quad |\eta_0| < \eta_2 \tag{38}$$

Note that for PWS maps of dimension two or higher, having the eigenvalues of the Jacobians on both sides of the border within the unit circle does not imply that the fixed points are the only attractors as μ is increased from negative values to positive values. In some situations, higher periodic attractors exist on one side or both sides of the border in addition to the stable fixed points. There is continuing effort by researchers to completely characterize the border collision bifurcations that occur in this parameter region when the eigenvalues of at least one of the Jacobians on either side of the border are nonreal. Sufficient conditions for having locally unique stable fixed points on both sides of the border are summarized in Section 2 (see also Figs. 1-2).

Although the focus of this paper is on using control to achieve certain safe, simple border collision bifurcations, it is deemed worthwhile to present the following two examples of more complex bifurcations. These examples show bifurcations of multiple attractors on one side or both sides of the border when the fixed point is stable on both sides of the border. Recently, it was shown that multiple attractor bifurcations are a source of unpredictability in piecewise smooth systems [10]. The presence of arbitrarily small noise may lead to fundamentally unpredictable behavior of orbits as a bifurcation parameter is varied slowly through a critical value.

Example 1 Stable fixed point plus period-4 attractor to stable fixed point plus period-3 attractor: Consider the following simple piecewise smooth linear 2D map

$$\begin{pmatrix} x_{k+1} \\ y_{k+1} \end{pmatrix} = \begin{cases} \begin{pmatrix} 0.50 & 1 \\ -0.90 & 0 \end{pmatrix} \begin{pmatrix} x_k \\ y_k \end{pmatrix} + \begin{pmatrix} 1 \\ 0 \end{pmatrix} \mu, & x_k \leq 0 \\ \begin{pmatrix} -1.22 & 1 \\ -0.36 & 0 \end{pmatrix} \begin{pmatrix} x_k \\ y_k \end{pmatrix} + \begin{pmatrix} 1 \\ 0 \end{pmatrix} \mu, & x_k > 0 \end{cases} \quad (39)$$

The map (39) undergoes a bifurcation from a stable fixed point plus period-4 attractor to a stable fixed point plus a period-3 attractor as μ is increased through zero (see Fig. 3 (a)). Note that the fixed point for $\mu < 0$ is spirally attracting ($\lambda_{L_{1,2}} = 0.25 \pm 0.9152i$) and for $\mu > 0$ is a flip attractor ($\lambda_{R_1} = -0.5, \lambda_{R_2} = -0.72$).

Example 2 Stable fixed point to stable fixed point plus period-7 attractor: Consider the following simple piecewise smooth linear 2D map

$$\begin{pmatrix} x_{k+1} \\ y_{k+1} \end{pmatrix} = \begin{cases} \begin{pmatrix} 1.6 & 1 \\ -0.8 & 0 \end{pmatrix} \begin{pmatrix} x_k \\ y_k \end{pmatrix} + \begin{pmatrix} 1 \\ 0 \end{pmatrix} \mu, & x_k \leq 0 \\ \begin{pmatrix} -1.4 & 1 \\ -0.6 & 0 \end{pmatrix} \begin{pmatrix} x_k \\ y_k \end{pmatrix} + \begin{pmatrix} 1 \\ 0 \end{pmatrix} \mu, & x_k > 0 \end{cases} \quad (40)$$

The map (40) undergoes a bifurcation from a stable fixed point to a stable fixed point plus a period-7 attractor as μ is increased through zero (see Fig. 3 (b)). Note that the fixed point for $\mu < 0$ is spirally attracting ($\lambda_{L_{1,2}} = 0.8 \pm 0.4i$) and for $\mu > 0$ is also spirally attracting with opposite sense of rotation ($\lambda_{R_{1,2}} = -0.7 \pm 0.3317i$).

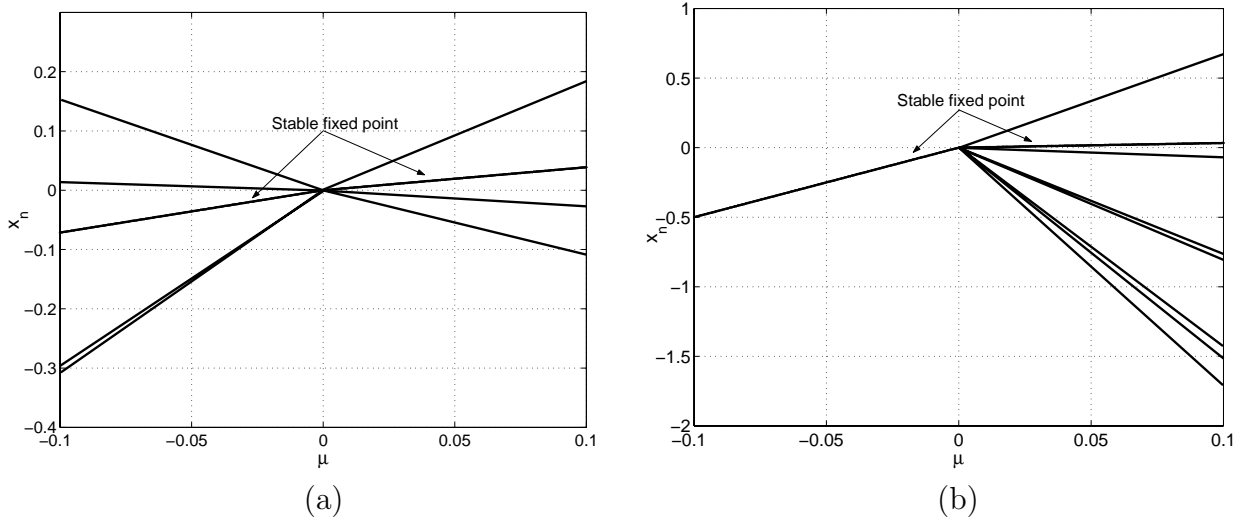


Figure 3: (a) Bifurcation diagram of (39) (b) Bifurcation diagram of (40).

In developing the control laws, the focus is on controlling “dangerous” border collision bifurcations and undesirable border collision bifurcations (see Section 2.6 for a list of dangerous and undesirable bifurcations).

3.1 Method 1: Control applied on one side of border

In this control scheme, the feedback control is applied only on one side of the border. Suppose that the system is operating at a stable fixed point on one side of the border, locally as the parameter approaches its critical value. Without loss of generality, assume this region of stable operation is R_L — that is, assume $-(1 + \delta_L) < \tau_L < (1 + \delta_L)$. Since the control is applied only on one side of the border, the linear state feedback can be applied either on the unstable side or the stable side of the border.

3.1.1 Linear feedback applied on the unstable side of the border

Recall that the fixed point is stable if it is in R_L and a BCB occurs as μ is increased through zero. Applying additive linear state feedback only for $(x, y) \in R_R$ leads to the closed-loop system

$$\begin{pmatrix} x_{k+1} \\ y_{k+1} \end{pmatrix} = \begin{cases} \begin{pmatrix} a_{11} & a_2 \\ a_{13} & a_4 \end{pmatrix} \begin{pmatrix} x_k \\ y_k \end{pmatrix} + \begin{pmatrix} \alpha_1 \\ \alpha_2 \end{pmatrix} \mu, & x_k \leq 0 \\ \begin{pmatrix} a_{21} & a_2 \\ a_{23} & a_4 \end{pmatrix} \begin{pmatrix} x_k \\ y_k \end{pmatrix} + \begin{pmatrix} \alpha_1 \\ \alpha_2 \end{pmatrix} \mu + \underbrace{\begin{pmatrix} b_1 \\ b_2 \end{pmatrix}}_{\mathbf{b}} u_k, & x_k > 0 \end{cases} \quad (41)$$

$$u_k = \underbrace{(\gamma_1 \ \gamma_2)}_{\mathbf{c}} \begin{pmatrix} x_k \\ y_k \end{pmatrix} = \gamma_1 x_k + \gamma_2 y_k \quad (42)$$

Suppose that the pair $(\mathbf{J}_R, \mathbf{b})$ is linearly reachable (i.e., the matrix $(\mathbf{b} \mid \mathbf{J}_R \mathbf{b})$ is nonsingular), then there exists a $\mathbf{c} = (\gamma_1 \ \gamma_2)$ such that the eigenvalues of the closed-loop matrix $\mathbf{J}_R + \mathbf{b}\mathbf{c}$ in R_R can be arbitrarily placed in the complex plane [32]. The characteristic equation of the Jacobian of the controlled system in the right side of the border is given by

$$\lambda^2 - \underbrace{(\tau_R + b_1\gamma_1 + b_2\gamma_2)}_{\tilde{\tau}_R} \lambda + \underbrace{\delta_R + (b_1 a_4 - a_2 b_2)\gamma_1 + (a_{21} b_2 - a_{23} b_1)\gamma_2}_{\tilde{\delta}_R} = 0 \quad (43)$$

where a tilde is used to denote variables that pertain to the closed loop system. Applying the Jury's test for second order systems, the fixed point to the right of the border for $\mu > 0$ is stable if and only if

$$-1 < \tilde{\delta}_R < 1 \quad (44)$$

$$1 + \tilde{\tau}_R + \tilde{\delta}_R > 0 \quad (45)$$

$$1 - \tilde{\tau}_R + \tilde{\delta}_R > 0 \quad (46)$$

Stability of the fixed point before the border for $\mu < 0$ and (44)-(46) is not sufficient to have locally unique attracting fixed points for negative and positive values of μ . To achieve locally unique fixed points and thus stabilize the BCB as μ is increased through zero, control gains are sought such that the parameters of the controlled system on both sides of the border are placed in one of the shaded regions of Figs. 1-2. Since the control has no effect on the

system to the left of the border (in R_L), the cases of real and complex eigenvalues of \mathbf{J}_L are considered separately.

Case 1: $\tau_L^2 \geq 4\delta_L$: This is tantamount to the eigenvalues being real (recall that $-(1 + \delta_L) < \tau_L < (1 + \delta_L)$), thus choosing the control gains such that $\tilde{\delta}_R < 0$ in (44)-(46) results in stabilizing the BCB. Note that this choice of the control gains places the controlled system parameters in the shaded region of Fig. 1 (b) if $\delta_L < 0$ and in one of shaded regions of Fig. 2 (a) if $\delta_L > 0$. Rewriting (44)-(46) and imposing $\tilde{\delta}_R < 0$ yields

$$(b_1 a_4 - a_2 b_2) \gamma_1 < -(a_{21} b_2 - a_{23} b_1) \gamma_2 - \delta_R \quad (47)$$

$$(b_1 a_4 - a_2 b_2) \gamma_1 > -(a_{21} b_2 - a_{23} b_1) \gamma_2 - \delta_R - 1 \quad (48)$$

$$(b_1 a_4 - a_2 b_2 + b_1) \gamma_1 > -(b_2 + a_{21} b_2 - a_{23} b_1) \gamma_2 - (1 + \tau_R + \delta_R) \quad (49)$$

$$(b_1 a_4 - a_2 b_2 - b_1) \gamma_1 > -(-b_2 + a_{21} b_2 - a_{23} b_1) \gamma_2 - (1 - \tau_R + \delta_R) \quad (50)$$

Stabilizing gains (γ_1, γ_2) can be obtained by finding the region in the (γ_1, γ_2) plane where inequalities (47)-(50) are satisfied. Such region is not empty, by the reachability assumption.

Case 2: $\tau_L^2 < 4\delta_L$: This is tantamount to the eigenvalues of \mathbf{J}_L being nonreal (i.e., the fixed point on the left hand side of the border for $\mu < 0$ is spirally attracting). Since control is applied on the unstable side only, it can modify the eigenvalues of \mathbf{J}_R but not those of \mathbf{J}_L . Thus, no control exists that can place the closed loop parameters in one of the shaded regions of Fig. 1 (a) or Fig. 2 (a). Therefore, it is concluded that when the fixed point in R_L for $\mu < 0$ is spirally attracting, one needs to apply the control on both sides of the border in order to stabilize the bifurcation and have a unique attracting fixed point on both sides of the border for negative and positive values of μ . This will be considered in a later section.

3.1.2 Linear feedback applied on the stable side of the border

For a linear state feedback applied on the stable side of the border to be effective in ensuring an acceptable bifurcation, it turns out that one must assume that the open-loop system supports a fixed point on the right side of the border for $\mu > 0$. This is tantamount to assuming $\tau_R < (1 + \delta_R)$. Of course, the assumption $-(1 + \delta_L) < \tau_L < (1 + \delta_L)$ is still in force. Consequently, this control method cannot be used to control border collision pair bifurcation. This method may be useful in controlling other types of BCB where the system supports a fixed point in R_R (e.g., bifurcation from a stable fixed point to chaos). Now, applying additive linear state feedback only for $(x, y) \in R_L$ yields the closed-loop system

$$\begin{pmatrix} x_{k+1} \\ y_{k+1} \end{pmatrix} = \begin{cases} \begin{pmatrix} a_{11} & a_2 \\ a_{13} & a_4 \end{pmatrix} \begin{pmatrix} x_k \\ y_k \end{pmatrix} + \begin{pmatrix} \alpha_1 \\ \alpha_2 \end{pmatrix} \mu + \underbrace{\begin{pmatrix} b_1 \\ b_2 \end{pmatrix}}_{\mathbf{b}} u_k, & x_k \leq 0 \\ \begin{pmatrix} a_{21} & a_2 \\ a_{23} & a_4 \end{pmatrix} \begin{pmatrix} x_k \\ y_k \end{pmatrix} + \begin{pmatrix} \alpha_1 \\ \alpha_2 \end{pmatrix} \mu, & x_k > 0 \end{cases} \quad (51)$$

$$u_k = \underbrace{(\gamma_1 \ \gamma_2)}_{\mathbf{c}} \begin{pmatrix} x_k \\ y_k \end{pmatrix} = \gamma_1 x_k + \gamma_2 y_k \quad (52)$$

Note that such a control scheme does not stabilize an unstable fixed point on the right side of the border for $\mu > 0$. This is because the control has no direct effect on the system for $(x, y) \in R_R$. All is not lost, however. It will be shown that this control scheme can be used to stabilize the BCB to a period-2 orbit.

The characteristic equation of the Jacobian of the controlled system to the left of the border is given by

$$\lambda^2 - \underbrace{(\tau_L + b_1\gamma_1 + b_2\gamma_2)}_{\tilde{\tau}_L} \lambda + \underbrace{\delta_L + (b_1a_4 - a_2b_2)\gamma_1 + (a_{11}b_2 - a_{13}b_1)\gamma_2}_{\tilde{\delta}_L} = 0 \quad (53)$$

To render the BCB a supercritical period doubling border collision, the fixed point to the left of the border must remain stable and the eigenvalues of the second iterate map with one point in R_L and the other point in R_R are inside the unit circle. Additional conditions are needed to ensure that the fixed point to the left of the border for $\mu < 0$ is a unique attractor and the period-2 orbit for $\mu > 0$ is also a unique attractor. The fixed point to the left of the border remains stable if and only if

$$-1 < \tilde{\delta}_L < 1 \quad (54)$$

$$1 + \tilde{\tau}_L + \tilde{\delta}_L > 0 \quad (55)$$

$$1 - \tilde{\tau}_L + \tilde{\delta}_L > 0 \quad (56)$$

The closed loop system (51)-(52) has a stable period-2 orbit for $\mu > 0$ if the eigenvalues of $(\mathbf{J}_L + \mathbf{bc})\mathbf{J}_R$ are inside the unit circle. It is straightforward to show that the characteristic polynomial of $(\mathbf{J}_L + \mathbf{bc})\mathbf{J}_R$ is

$$\lambda^2 - \tau_{12}\lambda + \delta_{12} = 0 \quad (57)$$

where

$$\tau_{12} = \underbrace{(a_{21}b_1 + a_2b_2)}_{\beta_1} \gamma_1 + \underbrace{(a_{23}b_1 + a_4b_2)}_{\beta_2} \gamma_2 + \underbrace{a_{11}a_{21} + a_4^2 + a_{23}a_2 + a_{13}a_2}_{\beta_3} \quad (58)$$

$$\begin{aligned} \delta_{12} = & \underbrace{(-a_2b_1a_4a_{23} + a_{23}a_2^2b_2 + a_{21}b_1a_4^2 - a_2a_4a_{21}b_2)}_{\beta_4} \gamma_1 \\ & + \underbrace{(-a_{11}a_2a_{23}b_2 - a_4b_1a_{13}a_{21} + a_{11}a_{21}a_4b_2 + b_1a_{23}a_{13}a_2)}_{\beta_5} \gamma_2 \\ & + \underbrace{(-a_{11}a_2a_4a_{23} + a_{23}a_2^2a_{13} - a_2a_4a_{13}a_{21} + a_{11}a_{21}a_4^2)}_{\beta_6} = 0 \end{aligned} \quad (59)$$

Applying the Jury's Test for second order systems, the period-2 orbit is stable iff

$$|\delta_{12}| < 1 \quad (60)$$

$$1 - \tau_{12} + \delta_{12} > 0 \quad (61)$$

$$1 + \tau_{12} + \delta_{12} > 0 \quad (62)$$

To make sure that no other attractors or repellers are involved in the BCB at $\mu = 0$, extra conditions need to be imposed. To this end, the cases when $\delta_R > 0$ and $\delta_R < 0$ are considered

separately (see Section 2 for details).

Case 1: $\delta_R < 0$: Achieving Scenario D

We seek control gains such that (54)-(56) and (60)-(62) are satisfied with $\tilde{\delta}_L < 0$. This gives a sufficient condition to have a unique attracting fixed point for $\mu < 0$ and a unique period-2 attractor for $\mu > 0$. Writing these conditions explicitly yields

$$(b_1 a_4 - a_2 b_2) \gamma_1 < -(a_{11} b_2 - a_{13} b_1) \gamma_2 - \delta_L \quad (63)$$

$$(b_1 a_4 - a_2 b_2) \gamma_1 > -(a_{11} b_2 - a_{13} b_1) \gamma_2 - \delta_L - 1 \quad (64)$$

$$(b_1 a_4 - a_2 b_2 + b_1) \gamma_1 > -(b_2 + a_{11} b_2 - a_{13} b_1) \gamma_2 - (1 + \tau_L + \delta_L) \quad (65)$$

$$(b_1 a_4 - a_2 b_2 - b_1) \gamma_1 > -(-b_2 + a_{11} b_2 - a_{13} b_1) \gamma_2 - (1 - \tau_L + \delta_L) \quad (66)$$

and

$$\beta_4 \gamma_1 < -\beta_5 \gamma_2 - \beta_6 + 1 \quad (67)$$

$$\beta_4 \gamma_1 > -\beta_5 \gamma_2 - \beta_6 - 1 \quad (68)$$

$$(-\beta_1 + \beta_4) \gamma_1 > (\beta_2 - \beta_5) \gamma_2 + \beta_3 - \beta_6 - 1 \quad (69)$$

$$(\beta_1 + \beta_4) \gamma_1 > -(\beta_2 + \beta_5) \gamma_2 - \beta_3 - \beta_6 - 1 \quad (70)$$

Case 2: $\delta_R > 0$

Since for positive determinants there are two regions in the parameter space where supercritical border collision period doubling occurs, different control laws will be needed to relocate the parameters to correspond to one of these regions (see Scenario B).

Case 2.1: Achieving Scenario B1

We seek control gains such that $0 < \tilde{\delta}_L < 1$, $-(1 + \tilde{\delta}_L) < \tilde{\tau}_L < -2\sqrt{\tilde{\delta}_L}$ and (60)-(62) are satisfied. This is a sufficient condition to have a unique attracting fixed point for $\mu < 0$ and a unique period-2 attractor for $\mu > 0$ (see Scenario B1). The conditions $0 < \tilde{\delta}_L < 1$ and $-(1 + \tilde{\delta}_L) < \tilde{\tau}_L < -2\sqrt{\tilde{\delta}_L}$ are satisfied if $0 < \tilde{\delta}_L < \epsilon$ and $-(1 + \tilde{\delta}_L) < \tilde{\tau}_L < -2\sqrt{\epsilon}$, where $\epsilon \in (0, 1)$. Here ϵ is a small parameter. It is used to simplify the conditions on the control gains and make the inequalities linear.

Writing these conditions explicitly yields

$$(b_1 a_4 - a_2 b_2) \gamma_1 < -(a_{11} b_2 - a_{13} b_1) \gamma_2 - \delta_L + \epsilon \quad (71)$$

$$(b_1 a_4 - a_2 b_2) \gamma_1 > -(a_{11} b_2 - a_{13} b_1) \gamma_2 - \delta_L \quad (72)$$

$$(b_1 a_4 - a_2 b_2 + b_1) \gamma_1 > -(b_2 + a_{11} b_2 - a_{13} b_1) \gamma_2 - (1 + \tau_L + \delta_L) \quad (73)$$

$$b_1 \gamma_1 < -b_2 \gamma_2 - \tau_L - 2\sqrt{\epsilon} \quad (74)$$

and

$$\beta_4 \gamma_1 < -\beta_5 \gamma_2 - \beta_6 + 1 \quad (75)$$

$$\beta_4 \gamma_1 > -\beta_5 \gamma_2 - \beta_6 - 1 \quad (76)$$

$$(-\beta_1 + \beta_4) \gamma_1 > (\beta_2 - \beta_5) \gamma_2 + \beta_3 - \beta_6 - 1 \quad (77)$$

Case 2.2: Achieving Scenario B2

We seek control gains such that $0 < \tilde{\delta}_L < 1$, $2\sqrt{\tilde{\delta}_L} < \tilde{\tau}_L < (1 + \tilde{\delta}_L)$ and (60)-(62) are satisfied. This is a sufficient condition to have a unique attracting fixed point for $\mu < 0$ and a unique period-2 attractor for $\mu > 0$ (see Scenario B2). The conditions $0 < \tilde{\delta}_L < 1$ and $2\sqrt{\tilde{\delta}_L} < \tilde{\tau}_L < (1 + \tilde{\delta}_L)$ are satisfied if $0 < \tilde{\delta}_L < \epsilon$ and $2\sqrt{\epsilon} < \tilde{\tau}_L < (1 + \tilde{\delta}_L)$, where $0 < \epsilon < 1$, small.

Writing these conditions explicitly yields

$$(b_1 a_4 - a_2 b_2) \gamma_1 < -(a_{11} b_2 - a_{13} b_1) \gamma_2 - \delta_L + \epsilon \quad (78)$$

$$(b_1 a_4 - a_2 b_2) \gamma_1 > -(a_{11} b_2 - a_{13} b_1) \gamma_2 - \delta_L \quad (79)$$

$$b_1 \gamma_1 > -b_2 \gamma_2 - \tau_L + 2\sqrt{\epsilon} \quad (80)$$

$$(b_1 a_4 - a_2 b_2 - b_1) \gamma_1 > -(-b_2 + a_{11} b_2 - a_{13} b_1) \gamma_2 - (1 - \tau_L + \delta_L) \quad (81)$$

and

$$\beta_4 \gamma_1 < -\beta_5 \gamma_2 - \beta_6 + 1 \quad (82)$$

$$\beta_4 \gamma_1 > -\beta_5 \gamma_2 - \beta_6 - 1 \quad (83)$$

$$(\beta_1 + \beta_4) \gamma_1 > -(\beta_2 + \beta_5) \gamma_2 - \beta_3 - \beta_6 - 1 \quad (84)$$

Stabilizing control gains can be obtained by finding the region in the (γ_1, γ_2) plane satisfied by inequalities (63)-(70) if $\delta_R < 0$ and inequalities (71)-(77) or (78)-(84) if $\delta_R > 0$.

3.2 Method 2: Different controls applied on each side of border

In this method, different controls are applied on each side of the border. Applying the linear state feedback additively in both the left and right sides of the border yields the closed-loop system

$$\begin{pmatrix} x_{k+1} \\ y_{k+1} \end{pmatrix} = \begin{cases} \begin{pmatrix} a_{11} & a_2 \\ a_{13} & a_4 \end{pmatrix} \begin{pmatrix} x_k \\ y_k \end{pmatrix} + \begin{pmatrix} \alpha_1 \\ \alpha_2 \end{pmatrix} \mu + \begin{pmatrix} b_1 \\ b_2 \end{pmatrix} u_{1k}, & x_k \leq 0 \\ \begin{pmatrix} a_{21} & a_2 \\ a_{23} & a_4 \end{pmatrix} \begin{pmatrix} x_k \\ y_k \end{pmatrix} + \begin{pmatrix} \alpha_1 \\ \alpha_2 \end{pmatrix} \mu + \begin{pmatrix} b_1 \\ b_2 \end{pmatrix} u_{2k}, & x_k > 0 \end{cases} \quad (85)$$

$$u_{1k} = (\gamma_{11} \ \gamma_{12}) \begin{pmatrix} x_k \\ y_k \end{pmatrix} = \gamma_{11} x_k + \gamma_{12} y_k \quad (86)$$

$$u_{2k} = (\gamma_{21} \ \gamma_{22}) \begin{pmatrix} x_k \\ y_k \end{pmatrix} = \gamma_{21} x_k + \gamma_{22} y_k \quad (87)$$

If the system linearizations on both sides of the border are reachable, then the BCB can be controlled to achieve any desired behavior. The fact that the controls on both sides are not equal provides the flexibility in placing the eigenvalues of the Jacobians of the system on both sides of the border to be in any desired locations. Obtaining stabilizing control gains for this case is straightforward. The drawback of this method is that knowledge of the border is needed in the design. If the location of the border is not exactly known, the control action may introduce complications into the system behavior.

3.3 Method 3: Simultaneous stabilization

In this method, the same linear state feedback control is applied additively on both the left and right sides of the border. This leads to the closed-loop system

$$\begin{pmatrix} x_{k+1} \\ y_{k+1} \end{pmatrix} = \begin{cases} \begin{pmatrix} a_{11} & a_2 \\ a_{13} & a_4 \end{pmatrix} \begin{pmatrix} x_k \\ y_k \end{pmatrix} + \begin{pmatrix} \alpha_1 \\ \alpha_2 \end{pmatrix} \mu + \begin{pmatrix} b_1 \\ b_2 \end{pmatrix} u_k, & x_k \leq 0 \\ \begin{pmatrix} a_{21} & a_2 \\ a_{23} & a_4 \end{pmatrix} \begin{pmatrix} x_k \\ y_k \end{pmatrix} + \begin{pmatrix} \alpha_1 \\ \alpha_2 \end{pmatrix} \mu + \begin{pmatrix} b_1 \\ b_2 \end{pmatrix} u_k, & x_k > 0 \end{cases} \quad (88)$$

$$u_k = (\gamma_1 \ \gamma_2) \begin{pmatrix} x_k \\ y_k \end{pmatrix} = \gamma_1 x_k + \gamma_2 y_k \quad (89)$$

Suppose that the fixed point to the left of the border for $\mu < 0$ is stable— that is, assume $-(1 + \delta_L) < \tau_L < (1 + \delta_L)$. Suppose also that as μ is increased through zero, a BCB occurs.

The characteristic polynomials of the closed loop system to the left and right of the border are given by

$$\tilde{p}_L(\lambda) = \lambda^2 - \underbrace{(\tau_L + b_1\gamma_1 + b_2\gamma_2)}_{\tilde{\tau}_L} \lambda + \underbrace{\delta_L + (b_1a_4 - a_2b_2)\gamma_1 + (a_{11}b_2 - a_{13}b_1)\gamma_2}_{\tilde{\delta}_L} = 0 \quad (90)$$

and

$$\tilde{p}_R(\lambda) = \lambda^2 - \underbrace{(\tau_R + b_1\gamma_1 + b_2\gamma_2)}_{\tilde{\tau}_R} \lambda + \underbrace{\delta_R + (b_1a_4 - a_2b_2)\gamma_1 + (a_{21}b_2 - a_{23}b_1)\gamma_2}_{\tilde{\delta}_R} = 0 \quad (91)$$

respectively.

A simultaneous control that renders the BCB to be from a locally unique stable fixed point to a locally unique stable fixed point exists if there is a (γ_1, γ_2) such that the parameters of the controlled system are in one of the shaded regions of Figs. 1-2. There is a total of nine different shaded regions in these figures. Next, conditions on the control gains that place the parameters of closed loop system in one of these regions are found. In all except one of the cases, the system of inequalities obtained isn't linear, and involves one or two square roots. By a parametrization technique, it is possible to obtain linear inequalities that imply the obtained inequalities. This is shown explicitly below only for Case 6; the other cases can be treated similarly.

Case 1: Placing parameters in upper right square of Fig. 1(a)

Control gain pairs (γ_1, γ_2) are sought such that

$$0 < \tilde{\delta}_L < 1 \quad \text{and} \quad 0 < \tilde{\delta}_R < 1 \\ 2\sqrt{\tilde{\delta}_L} < \tilde{\tau}_L < 1 + \tilde{\delta}_L \quad \text{and} \quad 2\sqrt{\tilde{\delta}_R} < \tilde{\tau}_R < 1 + \tilde{\delta}_R$$

Case 2: Placing parameters in upper left square of Fig. 1(a)

Control gain pairs (γ_1, γ_2) are sought such that

$$0 < \tilde{\delta}_L < 1 \quad \text{and} \quad 0 < \tilde{\delta}_R < 1 \\ -(1 + \tilde{\delta}_L) < \tilde{\tau}_L < -2\sqrt{\tilde{\delta}_L} \quad \text{and} \quad 2\sqrt{\tilde{\delta}_R} < \tilde{\tau}_R < 1 + \tilde{\delta}_R$$

Case 3: Placing parameters in lower left square of Fig. 1(a)

Control gain pairs (γ_1, γ_2) are sought such that

$$\begin{aligned} 0 < \tilde{\delta}_L < 1 & \quad \text{and} \quad 0 < \tilde{\delta}_R < 1 \\ -(1 + \tilde{\delta}_L) < \tilde{\tau}_L < -2\sqrt{\tilde{\delta}_L} & \quad \text{and} \quad -(1 + \tilde{\delta}_R) < \tilde{\tau}_R < -2\sqrt{\tilde{\delta}_R} \end{aligned}$$

Case 4: Placing parameters in lower right square of Fig. 1(a)

Control gain pairs (γ_1, γ_2) are sought such that

$$\begin{aligned} 0 < \tilde{\delta}_L < 1 & \quad \text{and} \quad 0 < \tilde{\delta}_R < 1 \\ 2\sqrt{\tilde{\delta}_L} < \tilde{\tau}_L < 1 + \tilde{\delta}_L & \quad \text{and} \quad -(1 + \tilde{\delta}_R) < \tilde{\tau}_R < -2\sqrt{\tilde{\delta}_R} \end{aligned}$$

Case 5: Placing parameters in shaded region of Fig. 1(b)

Control gain pairs (γ_1, γ_2) are sought such that

$$-1 < \tilde{\delta}_L < 0 \tag{92}$$

$$1 + \tilde{\tau}_L + \tilde{\delta}_L > 0 \tag{93}$$

$$1 - \tilde{\tau}_L + \tilde{\delta}_L > 0 \tag{94}$$

and

$$-1 < \tilde{\delta}_R < 0 \tag{95}$$

$$1 + \tilde{\tau}_R + \tilde{\delta}_R > 0 \tag{96}$$

$$1 - \tilde{\tau}_R + \tilde{\delta}_R > 0 \tag{97}$$

Substituting the expressions for $\tilde{\delta}_L$, $\tilde{\tau}_L$, $\tilde{\delta}_R$ and $\tilde{\tau}_R$ in (92)-(97) yields

$$(b_1 a_4 - a_2 b_2) \gamma_1 < -(a_{21} b_2 - a_{23} b_1) \gamma_2 - \delta_R \tag{98}$$

$$(b_1 a_4 - a_2 b_2) \gamma_1 > -(a_{21} b_2 - a_{23} b_1) \gamma_2 - \delta_R - 1 \tag{99}$$

$$(b_1 a_4 - a_2 b_2 + b_1) \gamma_1 > -(b_2 + a_{21} b_2 - a_{23} b_1) \gamma_2 - (1 + \tau_R + \delta_R) \tag{100}$$

$$(b_1 a_4 - a_2 b_2 - b_1) \gamma_1 > -(-b_2 + a_{21} b_2 - a_{23} b_1) \gamma_2 - (1 - \tau_R + \delta_R) \tag{101}$$

and

$$(b_1 a_4 - a_2 b_2) \gamma_1 < -(a_{11} b_2 - a_{13} b_1) \gamma_2 - \delta_L \tag{102}$$

$$(b_1 a_4 - a_2 b_2) \gamma_1 > -(a_{11} b_2 - a_{13} b_1) \gamma_2 - \delta_L - 1 \tag{103}$$

$$(b_1 a_4 - a_2 b_2 + b_1) \gamma_1 > -(b_2 + a_{11} b_2 - a_{13} b_1) \gamma_2 - (1 + \tau_L + \delta_L) \tag{104}$$

$$(b_1 a_4 - a_2 b_2 - b_1) \gamma_1 > -(-b_2 + a_{11} b_2 - a_{13} b_1) \gamma_2 - (1 - \tau_L + \delta_L) \tag{105}$$

Stabilizing control gains (if they exist) can be obtained by finding the region in the (γ_1, γ_2) plane satisfying inequalities (98)-(105).

Case 6: Placing parameters in left rectangle of Fig. 2(a)

Control gain pairs (γ_1, γ_2) are sought such that

$$0 < \tilde{\delta}_L < 1 \tag{106}$$

$$-(1 + \tilde{\delta}_L) < \tilde{\tau}_L < -2\sqrt{\tilde{\delta}_L} \tag{107}$$

and

$$-1 < \tilde{\delta}_R < 1 \quad (108)$$

$$-(1 + \tilde{\delta}_R) < \tilde{\tau}_R < (1 + \tilde{\delta}_R) \quad (109)$$

Explicit conditions on the control gains can be obtained as follows: Introduce a small parameter $\epsilon \in (0, 1)$. Seek control gains such that $0 < \tilde{\delta}_L < \epsilon$ and $-(1 + \tilde{\delta}_L) < \tilde{\tau}_L < -2\sqrt{\epsilon}$. Then (106)-(109) yield

$$(b_1 a_4 - a_2 b_2) \gamma_1 < -(a_{11} b_2 - a_{13} b_1) \gamma_2 - \delta_L + \epsilon \quad (110)$$

$$(b_1 a_4 - a_2 b_2) \gamma_1 > -(a_{11} b_2 - a_{13} b_1) \gamma_2 - \delta_L \quad (111)$$

$$(b_1 a_4 - a_2 b_2 + b_1) \gamma_1 > -(b_2 + a_{11} b_2 - a_{13} b_1) \gamma_2 - (1 + \tau_L + \delta_L) \quad (112)$$

$$b_1 \gamma_1 < -b_2 \gamma_2 - \tau_L - 2\sqrt{\epsilon} \quad (113)$$

and

$$(b_1 a_4 - a_2 b_2) \gamma_1 < -(a_{21} b_2 - a_{23} b_1) \gamma_2 - \delta_R + 1 \quad (114)$$

$$(b_1 a_4 - a_2 b_2) \gamma_1 > -(a_{21} b_2 - a_{23} b_1) \gamma_2 - \delta_R - 1 \quad (115)$$

$$(b_1 a_4 - a_2 b_2 + b_1) \gamma_1 > -(b_2 + a_{21} b_2 - a_{23} b_1) \gamma_2 - (1 + \tau_R + \delta_R) \quad (116)$$

$$(b_1 a_4 - a_2 b_2 - b_1) \gamma_1 > -(-b_2 + a_{21} b_2 - a_{23} b_1) \gamma_2 - (1 - \tau_R + \delta_R) \quad (117)$$

Case 7: Placing parameters in right rectangle of Fig. 2(a)

Control gain pairs (γ_1, γ_2) are sought such that

$$\begin{aligned} 0 < \tilde{\delta}_L < 1 \\ 2\sqrt{\tilde{\delta}_L} < \tilde{\tau}_L < 1 + \tilde{\delta}_L \end{aligned} \quad \text{and} \quad \begin{aligned} -1 < \tilde{\delta}_R < 1 \\ -(1 + \tilde{\delta}_R) < \tilde{\tau}_R < -(1 + \tilde{\delta}_R) \end{aligned}$$

Case 8: Placing parameters in upper rectangle of Fig. 2(b)

Control gain pairs (γ_1, γ_2) are sought such that

$$\begin{aligned} -1 < \tilde{\delta}_L < 1 \\ -(1 + \tilde{\delta}_L) < \tilde{\tau}_L < (1 + \tilde{\delta}_L) \end{aligned} \quad \text{and} \quad \begin{aligned} 0 < \tilde{\delta}_R < 1 \\ 2\sqrt{\tilde{\delta}_R} < \tilde{\tau}_R < 1 + \tilde{\delta}_R \end{aligned}$$

Case 9: Placing parameters in lower rectangle of Fig. 2(b)

Control gain pairs (γ_1, γ_2) are sought such that

$$\begin{aligned} -1 < \tilde{\delta}_L < 1 \\ -(1 + \tilde{\delta}_L) < \tilde{\tau}_L < (1 + \tilde{\delta}_L) \end{aligned} \quad \text{and} \quad \begin{aligned} 0 < \tilde{\delta}_R < 1 \\ -(1 + \tilde{\delta}_R) < \tilde{\tau}_R < -2\sqrt{\tilde{\delta}_R} \end{aligned}$$

The next example illustrates how the developed control laws can be used to control border collision bifurcation.

Example 3 Border collision pair bifurcation (saddle node bifurcation)

Consider the following simple piecewise smooth linear 2D map

$$\begin{pmatrix} x_{k+1} \\ y_{k+1} \end{pmatrix} = \begin{cases} \underbrace{\begin{pmatrix} 1 & 1 \\ -0.5 & 0 \end{pmatrix}}_{\mathbf{J}_L} \begin{pmatrix} x_k \\ y_k \end{pmatrix} + \begin{pmatrix} 1 \\ 0 \end{pmatrix} \mu + \begin{pmatrix} 1 \\ 0 \end{pmatrix} u_k, & x_k \leq 0 \\ \underbrace{\begin{pmatrix} 2.5 & 1 \\ -0.7 & 0 \end{pmatrix}}_{\mathbf{J}_R} \begin{pmatrix} x_k \\ y_k \end{pmatrix} + \begin{pmatrix} 1 \\ 0 \end{pmatrix} \mu + \begin{pmatrix} 1 \\ 0 \end{pmatrix} u_k, & x_k > 0 \end{cases} \quad (118)$$

$$u_k = \gamma_1 x_k + \gamma_2 y_k \quad (119)$$

The map (118) with $u_k = 0$ undergoes a border collision pair bifurcation (saddle node bifurcation), where a stable and an unstable fixed point merge and disappear as μ is increased through zero (see Fig. 4). This is an example of a “dangerous” bifurcation. For this example, $a_{11} = 1$, $a_2 = 1$, $a_{13} = -0.5$, $a_4 = 0$, $a_{21} = -2.5$, $a_{23} = -0.7$, $\alpha_1 = 1$ and $\alpha_2 = 0$. The eigenvalues of \mathbf{J}_L are $\lambda_{L1,2} = 0.5 \pm 0.5i$ and those of \mathbf{J}_R are $\lambda_{R1} = 2.1787$ and $\lambda_{R2} = 0.3213$.

Next, the control methods developed above are applied to control the BCB in (118) so that the closed loop system possesses a locally unique and attracting fixed point on both sides of the border.

Control applied on unstable side

Control applied on the unstable side does not exist for this example since the eigenvalues of \mathbf{J}_L are complex ($\tau_L^2 < 4\delta_L$).

Control applied on stable side

Recall that for a control applied on the stable side to be effective in ensuring an acceptable bifurcation, the uncontrolled system must support a fixed point to the right side of the border for positive values of μ . Since in this example, no fixed point exists for $\mu > 0$, stable side control does not work.

Different controls applied on each side of the border

Since the control on the left side of the border can be chosen independently of that to the right of the border (as long as the controlled system parameters lie within one of the shaded regions of Figs. 1-2), the border collision pair bifurcation can be controlled to achieve a transition from a stable fixed point to a stable fixed point as μ is increased through zero. The calculations are trivial for this case and thus are not presented.

Simultaneous control

For this example, it is straightforward to check that there are control gains that satisfy inequalities (98)-(105). Thus, the controlled system parameters can be placed in the shaded region of Fig. 1(b). A set of stabilizing control gain pairs (γ_1, γ_2) is obtained from inequalities (98)-(105) and is depicted in Fig. 5 (a). The bifurcation diagram of the controlled system with $\gamma_1 = -1.95$ and $\gamma_2 = -1.05$ is shown in Fig. 5 (b).

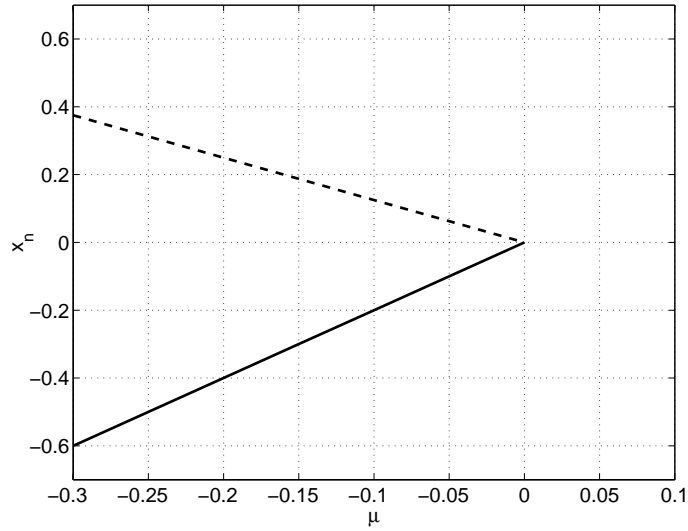


Figure 4: Bifurcation diagram of uncontrolled system (118). A solid line represents a path of stable fixed points whereas a dashed line represents a path of unstable fixed points.

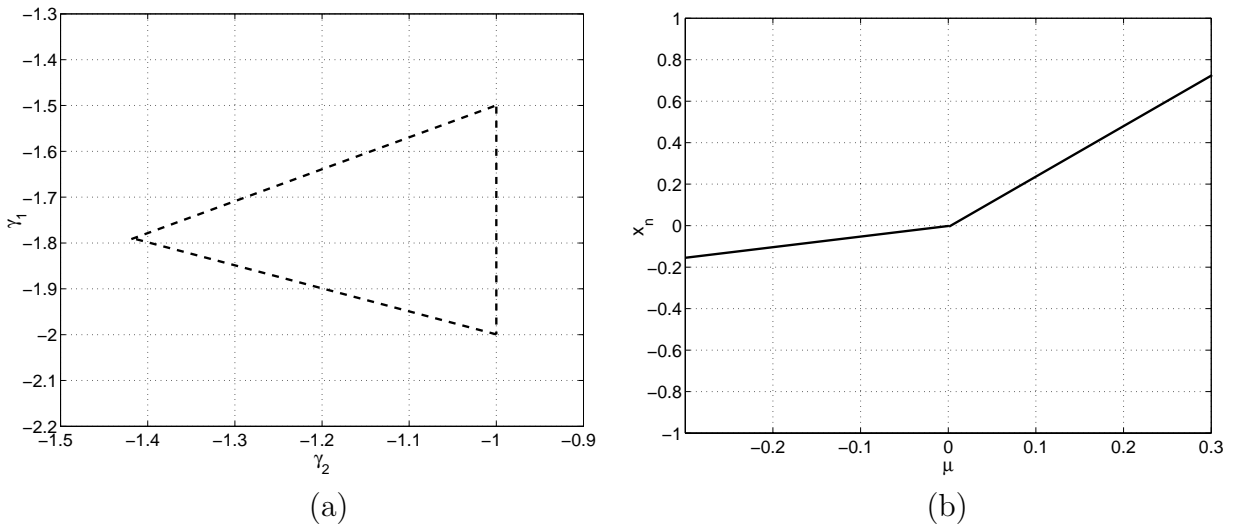


Figure 5: (a) The interior of the triangle gives simultaneously stabilizing control gains for (118)-(119) (b) Bifurcation diagram of a simultaneously controlled system (118)-(119) using $\gamma_1 = -1.95$ and $\gamma_2 = -1.05$. A locally unique and stable fixed point exists on both sides of the border.

4 Quenching of a Period Doubling BCB in a Cardiac Conduction Model

In this section, we consider a cardiac conduction model that was proposed by Sun et al. [25]. The model incorporates physiological concepts of recovery, facilitation and fatigue. It is formulated as a two-dimensional PWS map. Two factors determine the atrioventricular (AV) nodal conduction time: the time interval from the atrial activation to the activation of the Bundle of His and the history of activation of the node. The model predicts a variety of experimentally observed complex rhythms of nodal conduction. In particular, alternans rhythms, in which there is an alternation in conduction time from beat to beat, are associated with period-doubling bifurcation in the theoretical model.

The authors first define the atrial His interval, A , to be that between cardiac impulse excitation of the lower interatrial septum to the Bundle of His. (See [25] for definitions.) The model is:

$$\begin{pmatrix} A_{n+1} \\ R_{n+1} \end{pmatrix} = f(A_n, R_n, H_n)$$

where

$$f(A_n, R_n, H_n) = \begin{cases} \begin{pmatrix} A_{min} + R_{n+1} + (201 - 0.7A_n)e^{-H_n/\tau_{rec}} \\ R_n e^{-(A_n+H_n)/\tau_{fat}} + \gamma e^{-H_n/\tau_{fat}} \end{pmatrix}, & \text{for } A_n \leq 130 \\ \begin{pmatrix} A_{min} + R_{n+1} + (500 - 3.0A_n)e^{-H_n/\tau_{rec}} \\ R_n e^{-(A_n+H_n)/\tau_{fat}} + \gamma e^{-H_n/\tau_{fat}} \end{pmatrix}, & \text{for } A_n > 130 \end{cases} \quad (120)$$

with $R_0 = \gamma \exp(-H_0/\tau_{fat})$. Here H_0 is the initial H interval and the parameters A_{min} , τ_{fat} , γ and τ_{rec} are positive constants. The variable H_n represents the interval between bundle of His activation and the subsequent activation (the AV nodal recovery time) and is usually taken as the bifurcation parameter. The variable R_n represents a drift in the nodal conduction time, and is sometimes taken to be constant. In this section, we consider R_n as a variable as in [25]. Note that the map f is piecewise smooth and is continuous at the border $A_b := 130$ ms.

Several researchers studied this model and developed control techniques to stabilize the unstable fixed point (e.g., [33, 34, 35, 36]). With the exception of [36], all the studies of this model reported in the literature viewed the border collision period doubling bifurcation in this system as if it were an ordinary period doubling bifurcation in a smooth dynamical system. Although in [36] the bifurcation in the cardiac model was recognized as a border collision, the control design proposed there was based on bifurcation control results for smooth systems. They used a linear feedback with control gain determined by trial and error. In [34], the authors propose the use of linear delay feedback to suppress the period doubling bifurcation. In [33], the authors apply control of chaos technique to suppress the alternation resulting from the period doubling bifurcation. In this work, we show that the period doubling bifurcation is an instance of a BCB and apply the control techniques developed in this paper to quench the period doubling BCB, and simultaneously stabilize the fixed point after the border.

4.1 Analysis of the border collision bifurcation

Numerical simulations show that the map (120) undergoes a supercritical period doubling bifurcation as the bifurcation parameter $S := H_n$ is decreased through a critical value (see Fig. 6). We show that this bifurcation is a supercritical period doubling BCB which occurs as the fixed point of the map hits the border $A_b = 130$.

Let the fixed points of the map (120) be given by $(A_1^*(S), R_1^*(S))$ for $A_n < A_b$ and $(A_2^*(S), R_2^*(S))$ for $A_n > A_b$. Under normal conditions, the fixed point $(A_1^*(S), R_1^*(S))$ is stable and it loses stability as S is decreased through a critical value $S = S_b$ where $A_1^* = A_b$. Then, at S_b , $R_1^* := R_b$.

Next, a change of variable is introduced such that the fixed point is at the origin at $S = 0$. Let $\bar{A}_n = A_n - A_b = A_n - 130$, $\bar{R}_n = R_n - R_b$ and $\bar{S} = S - S_b$. The map becomes

$$\bar{f}(\bar{A}_n, \bar{R}_n, \bar{S}) = \begin{cases} \begin{pmatrix} A_{min} + \bar{R}_{n+1} + (110 - 0.7\bar{A}_n)e^{\frac{-(\bar{S}+S_b)}{\tau_{rec}}} - 130 \\ (\bar{R}_n + R_b)e^{\frac{-(\bar{A}_n+130+\bar{S}+S_b)}{\tau_{fat}}} + \gamma e^{\frac{-(\bar{S}+S_b)}{\tau_{fat}}} \end{pmatrix}, & \text{for } \bar{A}_n \leq 0 \\ \begin{pmatrix} A_{min} + \bar{R}_{n+1} + (110 - 3.0\bar{A}_n)e^{\frac{-(\bar{S}+S_b)}{\tau_{rec}}} - 130 \\ (\bar{R}_n + R_b)e^{\frac{-(\bar{A}_n+130+\bar{S}+S_b)}{\tau_{fat}}} + \gamma e^{\frac{-(\bar{S}+S_b)}{\tau_{fat}}} \end{pmatrix}, & \text{for } \bar{A}_n > 0 \end{cases} \quad (121)$$

The Jacobians to the left of the border close to the origin \mathbf{J}_L and to the right of the border close to the origin \mathbf{J}_R are given by

$$\mathbf{J}_L = \begin{pmatrix} -0.7e^{\frac{-S_b}{\tau_{rec}}} - \frac{R_b}{\tau_{fat}}e^{\frac{-(130+S_b)}{\tau_{fat}}} & e^{\frac{-(130+S_b)}{\tau_{fat}}} \\ -\frac{R_b}{\tau_{fat}}e^{\frac{-(130+S_b)}{\tau_{fat}}} & e^{\frac{-(130+S_b)}{\tau_{fat}}} \end{pmatrix} \quad (122)$$

and

$$\mathbf{J}_R = \begin{pmatrix} -3.0e^{\frac{-S_b}{\tau_{rec}}} - \frac{R_b}{\tau_{fat}}e^{\frac{-(130+S_b)}{\tau_{fat}}} & e^{\frac{-(130+S_b)}{\tau_{fat}}} \\ -\frac{R_b}{\tau_{fat}}e^{\frac{-(130+S_b)}{\tau_{fat}}} & e^{\frac{-(130+S_b)}{\tau_{fat}}} \end{pmatrix} \quad (123)$$

respectively. Also, the derivative of f with respect to S is

$$\begin{pmatrix} \alpha_1 \\ \alpha_2 \end{pmatrix} = \begin{pmatrix} -\frac{110}{\tau_{rec}}e^{\frac{-S_b}{\tau_{rec}}} - \frac{\gamma}{\tau_{fat}}e^{\frac{-S_b}{\tau_{fat}}} - \frac{R_b}{\tau_{fat}}e^{\frac{-(130+S_b)}{\tau_{fat}}} \\ -\frac{\gamma}{\tau_{fat}}e^{\frac{-S_b}{\tau_{fat}}} - \frac{R_b}{\tau_{fat}}e^{\frac{-(130+S_b)}{\tau_{fat}}} \end{pmatrix} \quad (124)$$

Next, the following parameter values are assumed (borrowed from [25]): $\tau_{rec} = 70\text{ms}$, $\tau_{fat} = 30000\text{ms}$, $A_{min} = 33\text{ms}$, $\gamma = 0.3\text{ms}$. For these parameter values, $S_b = 56.9078\text{ms}$, $R_b = 48.2108\text{ms}$ and

$$\mathbf{J}_L = \begin{pmatrix} -0.31208 & 0.99379 \\ -0.001597 & 0.99379 \end{pmatrix}, \quad \mathbf{J}_R = \begin{pmatrix} -1.33223 & 0.99379 \\ -0.001597 & 0.99379 \end{pmatrix}$$

and

$$\begin{pmatrix} \alpha_1 \\ \alpha_2 \end{pmatrix} = \begin{pmatrix} -0.69861 \\ -0.001607 \end{pmatrix}.$$

The eigenvalues of \mathbf{J}_L are $\lambda_{L1} = -0.3109$, $\lambda_{L2} = 0.9926$ ($\tau_L = 0.6817$, $\delta_L = -0.3086$) and those of \mathbf{J}_R are $\lambda_{R1} = -1.3315$, $\lambda_{R2} = 0.9931$ ($\tau_R = -0.3384$ and $\delta_R = -1.3224$). Note that there is a discontinuous jump in the eigenvalues at the border collision bifurcation. The stability of the period-2 orbit with one point in R_L and the other in R_R is determined by the eigenvalues of $\mathbf{J}_{LR} := \mathbf{J}_L \mathbf{J}_R$. These eigenvalues are $\lambda_{LR1} = 0.4135$ and $\lambda_{LR2} = 0.9867$. This implies that a stable period-2 orbit is born after the border collision as seen in the simulations.

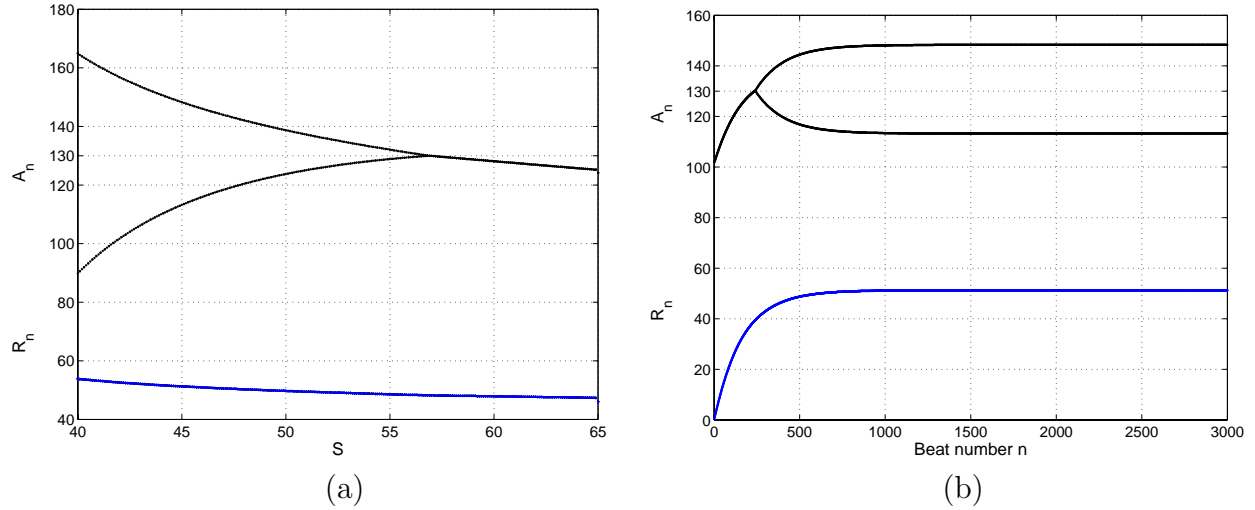


Figure 6: (a) Joint bifurcation diagram for A_n and for R_n for (120) with S as bifurcation parameter and $\tau_{rec} = 70\text{ms}$, $\tau_{fat} = 30000\text{ms}$, $A_{min} = 33\text{ms}$ and $\gamma = 0.3\text{ms}$ (b) Iterations of map showing the alternation in A_n as a result of a period doubling bifurcation. The parameter values are the same as in (a) with $S = 45\text{ms}$.

4.2 Feedback control of border collision bifurcation

For the cardiac conduction model, the control is usually applied as a perturbation to the bifurcation parameter \bar{S} [33, 36]. The control methods developed in this paper are used to quench the period doubling bifurcation. Static feedback applied on the stable side only cannot stabilize an unstable fixed point on the other side of the border. However, it can be used to reduce the amplitude of the bifurcated period-2 orbit. This is not pursued here, since we are interested in quenching the period-2 orbit.

Next, static feedback applied on the unstable side is considered followed by simultaneous control.

4.2.1 Static feedback applied on unstable side

Applying static linear state feedback on the unstable side only ($\bar{A}_n > 0$) as a perturbation to the bifurcation parameter yields the closed loop system

$$\begin{pmatrix} \bar{A}_{n+1} \\ \bar{R}_{n+1} \end{pmatrix} = \begin{cases} \begin{pmatrix} A_{min} + \bar{R}_{n+1} + (110 - 0.7\bar{A}_n)e^{\frac{-(\bar{S}+S_b)}{\tau_{rec}}} - 130 \\ (\bar{R}_n + R_b)e^{\frac{-(\bar{A}_n+130+\bar{S}+S_b)}{\tau_{fat}}} + \gamma e^{\frac{-(\bar{S}+S_b)}{\tau_{fat}}} \end{pmatrix}, & \text{for } \bar{A}_n \leq 0 \\ \begin{pmatrix} A_{min} + \bar{R}_{n+1} + (110 - 3\bar{A}_n)e^{\frac{-(\bar{S}+S_b+u_n)}{\tau_{rec}}} - 130 \\ (\bar{R}_n + R_b)e^{\frac{-(\bar{A}_n+130+\bar{S}+S_b+u_n)}{\tau_{fat}}} + \gamma e^{\frac{-(\bar{S}+S_b+u_n)}{\tau_{fat}}} \end{pmatrix}, & \text{for } \bar{A}_n > 0 \end{cases} \quad (125)$$

$$u_n = (\gamma_1 \ \gamma_2) \begin{pmatrix} \bar{A}_n \\ \bar{R}_n \end{pmatrix} = \gamma_1 \bar{A}_n + \gamma_2 \bar{R}_n \quad (126)$$

For the assumed parameter values, the Jacobians for $\bar{A}_n < 0$ and $\bar{A}_n > 0$ are

$$\tilde{\mathbf{J}}_{\mathbf{L}} = \mathbf{J}_L = \begin{pmatrix} -0.31208 & 0.99379 \\ -0.001597 & 0.99379 \end{pmatrix},$$

and

$$\begin{aligned} \tilde{\mathbf{J}}_{\mathbf{R}} &= \begin{pmatrix} -1.33223 - 0.69860\gamma_1 & 0.99379 - 0.69860\gamma_2 \\ -0.001597 - 0.001607\gamma_1 & 0.99379 - 0.001607\gamma_2 \end{pmatrix} \\ &= \underbrace{\begin{pmatrix} -1.33223 & 0.99379 \\ -0.001597 & 0.99379 \end{pmatrix}}_{\mathbf{J}_R} + \underbrace{\begin{pmatrix} -0.69860 \\ -0.001607 \end{pmatrix}}_{\mathbf{b}} \begin{pmatrix} \gamma_1 & \gamma_2 \end{pmatrix} \end{aligned}$$

respectively. Using the results of Section 3.1.1 Case 1, stabilizing control gains (γ_1, γ_2) are obtained by solving (47)-(50). Figure 7 (a) shows all the possible stabilizing gains (γ_1, γ_2) that satisfy (47)-(50), and Fig. 7 (b) shows the bifurcation diagram of the controlled system with $(\gamma_1, \gamma_2) = (-1, 0)$. Note that by setting $\gamma_2 = 0$, only A_n is used in the feedback. In practice, the conduction time of the n th beat A_n , can be measured. The state A_n has been used in the feedback loop by other researchers who developed control laws for this model (e.g., [34, 36]).

4.2.2 Simultaneous static feedback control

Applying the same static linear state feedback on both sides of the border as a perturbation to the bifurcation parameter yields the closed loop system

$$\begin{pmatrix} \bar{A}_{n+1} \\ \bar{R}_{n+1} \end{pmatrix} = \begin{cases} \begin{pmatrix} A_{min} + \bar{R}_{n+1} + (110 - 0.7\bar{A}_n)e^{\frac{-(\bar{S}+S_b+u_n)}{\tau_{rec}}} - 130 \\ (\bar{R}_n + R_b)e^{\frac{-(\bar{A}_n+130+\bar{S}+S_b+u_n)}{\tau_{fat}}} + \gamma e^{\frac{-(\bar{S}+S_b+u_n)}{\tau_{fat}}} \end{pmatrix}, & \text{for } \bar{A}_n \leq 0 \\ \begin{pmatrix} A_{min} + \bar{R}_{n+1} + (110 - 3\bar{A}_n)e^{\frac{-(\bar{S}+S_b+u_n)}{\tau_{rec}}} - 130 \\ (\bar{R}_n + R_b)e^{\frac{-(\bar{A}_n+130+\bar{S}+S_b+u_n)}{\tau_{fat}}} + \gamma e^{\frac{-(\bar{S}+S_b+u_n)}{\tau_{fat}}} \end{pmatrix}, & \text{for } \bar{A}_n > 0 \end{cases} \quad (127)$$

$$u_n = (\gamma_1 \ \gamma_2) \begin{pmatrix} \bar{A}_n \\ \bar{R}_n \end{pmatrix} = \gamma_1 \bar{A}_n + \gamma_2 \bar{R}_n \quad (128)$$

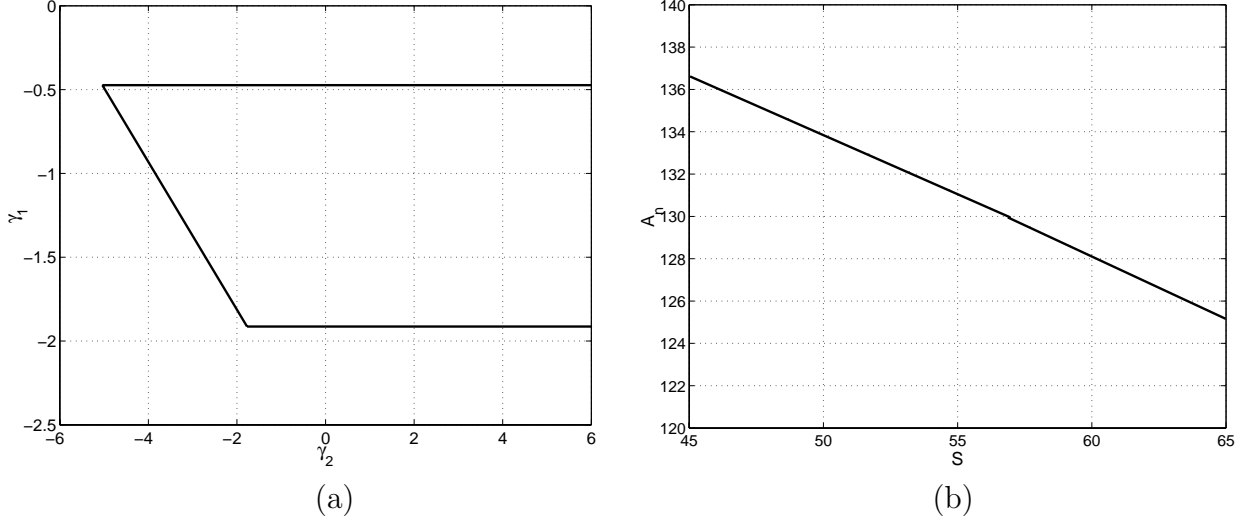


Figure 7: (a) Stabilizing control gain pairs satisfying (47)-(50) are within the region subtended by the lines in the figure, with static linear state feedback control applied on unstable side ($A_n > 130$) (b) Bifurcation diagram of the controlled system using static linear state feedback applied in the unstable region with control gains $(\gamma_1, \gamma_2) = (-1, 0)$.

The Jacobians of the controlled system to the left and right of the border are given by

$$\begin{aligned} \tilde{\mathbf{J}}_{\mathbf{L}} &= \begin{pmatrix} -0.31208 - 0.69860\gamma_1 & 0.99379 - 0.69860\gamma_2 \\ -0.001597 - 0.001607\gamma_1 & 0.99379 - 0.001607\gamma_2 \end{pmatrix} \\ &= \underbrace{\begin{pmatrix} -0.31208 & 0.99379 \\ -0.001597 & 0.99379 \end{pmatrix}}_{\mathbf{J}_{\mathbf{L}}} + \underbrace{\begin{pmatrix} -0.69860 \\ -0.001607 \end{pmatrix}}_{\mathbf{b}} \begin{pmatrix} \gamma_1 & \gamma_2 \end{pmatrix} \end{aligned}$$

and

$$\begin{aligned} \tilde{\mathbf{J}}_{\mathbf{R}} &= \begin{pmatrix} -1.33223 - 0.69860\gamma_1 & 0.99379 - 0.69860\gamma_2 \\ -0.001597 - 0.001607\gamma_1 & 0.99379 - 0.001607\gamma_2 \end{pmatrix} \\ &= \underbrace{\begin{pmatrix} -1.33223 & 0.99379 \\ -0.001597 & 0.99379 \end{pmatrix}}_{\mathbf{J}_{\mathbf{R}}} + \begin{pmatrix} -0.69860 \\ -0.001607 \end{pmatrix} \begin{pmatrix} \gamma_1 & \gamma_2 \end{pmatrix} \end{aligned}$$

respectively. Using the results of Section 3.3, Case 5, stabilizing control gains (γ_1, γ_2) are obtained by solving (98)-(105). Figure 8 (a) shows all stabilizing gains (γ_1, γ_2) that satisfy (98)-(105), and Fig. 8 (b) shows the bifurcation diagram of the controlled system with $(\gamma_1, \gamma_2) = (-1, 0)$. Figure 9 shows the effectiveness of the control in quenching the period-2 orbit and simultaneously stabilizing the unstable fixed point.

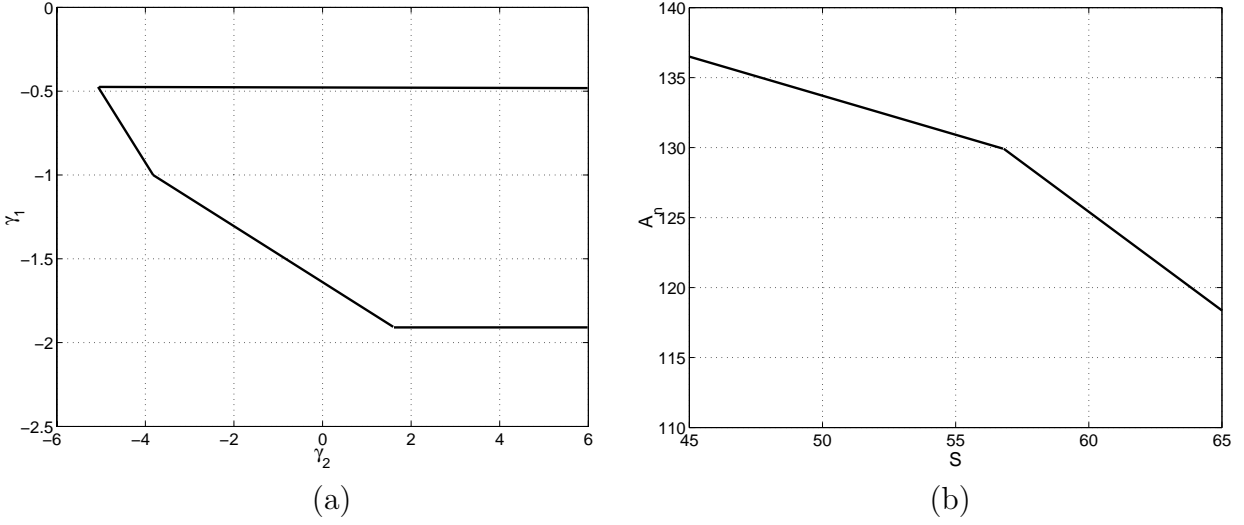


Figure 8: (a) Stabilizing control gain pairs satisfying (98)-(105) are within the region subtended by the lines in the figure, with simultaneous static linear state feedback control (b) Bifurcation diagram of the controlled system using simultaneous static linear state feedback with control gains $(\gamma_1, \gamma_2) = (-1, 0)$.

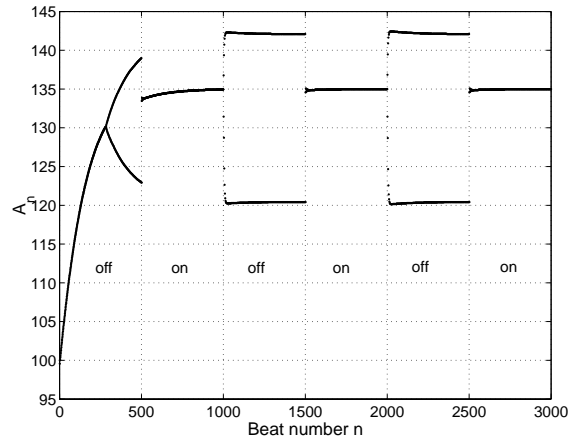


Figure 9: Iterations of map. Simultaneous static linear state feedback control applied at beat number $n = 500$. The control is switched off and on every 500 beats to show the effectiveness of the controller. Here $S = 48\text{ms}$ and $(\gamma_1, \gamma_2) = (-1, 0)$.

Acknowledgement

This work was supported in part by the National Science Foundation under Grant Number ECS-0115160. The authors are grateful to Dr. James Bailey of the National Institutes of Health for helpful discussions on the example of Section 4.

References

- [1] M.A. Hassouneh, E.H. Abed, and S. Banerjee, “Feedback control of border collision bifurcations in one dimensional piecewise smooth maps,” Submitted.
- [2] M.A. Hassouneh and E.H. Abed, “Feedback control of border collision bifurcations in piecewise smooth maps,” Tech. Rep. TR 2002-26, ISR, University of Maryland, College Park, April 2002.
- [3] H. E. Nusse and J. A. Yorke, “Border-collision bifurcations including “period two to period three” for piecewise smooth maps,” *Physica D*, vol. 57, pp. 39–57, 1992.
- [4] M. I. Feigin, “Doubling of the oscillation period with c -bifurcations in piecewise continuous systems,” *Prikladnaya Matematika i Mekhanika*, vol. 34, pp. 861–869, 1970.
- [5] M. di Bernardo, M. I. Feigin, S. J. Hogan, and M. E. Homer, “Local analysis of C -bifurcations in n -dimensional piecewise smooth dynamical systems,” *Chaos, Solitons & Fractals*, vol. 10, no. 11, pp. 1881–1908, 1999.
- [6] H. E. Nusse and J. A. Yorke, “Border-collision bifurcations for piecewise smooth one-dimensional maps,” *International Journal of Bifurcation & Chaos*, vol. 5, pp. 189–207, 1995.
- [7] S. Banerjee, M. S. Karthik, G. H. Yuan, and J. A. Yorke, “Bifurcations in one-dimensional piecewise smooth maps- theory and applications in switching systems,” *IEEE Transactions on Circuits and Systems I*, vol. 47, no. 3, pp. 389–394, 2000.
- [8] S. Banerjee and C. Grebogi, “Border collision bifurcations in two-dimensional piecewise smooth maps,” *Physical Review E*, vol. 59, no. 4, pp. 4052–4061, 1999.
- [9] S. Banerjee, J. A. Yorke, and C. Grebogi, “Robust chaos,” *Physical Review Letters*, vol. 80, pp. 3049–3052, April 1998.
- [10] M. Dutta et al., “Multiple attractor bifurcations: A source of unpredictability in piecewise smooth systems,” *Physical Review Letters*, vol. 83, no. 21, pp. 4281–4284, Nov 1999.
- [11] M. di Bernardo, C.J. Budd, and A.R. Champneys, “Corner collision implies border-collision bifurcation,” *Physica D*, vol. 154, pp. 171–194, 2001.
- [12] C.S. Hsu, E. Kreuzer, and M.C. Kim, “Bifurcation characteristics of piecewise linear mappings and their applications,” *Dynamics and Stability of Systems*, vol. 5, no. 4, pp. 227–254, 1990.

- [13] H. E. Nusse, E. Ott, and J. A. Yorke, “Border-collision bifurcation: An explanation for an observed phenomena,” *Physical Review E*, vol. 201, pp. 197–204, 1994.
- [14] M. Ohnishi and N. Inaba, “A singular bifurcation into instant chaos in piecewise-linear circuit,” *IEEE Transactions on Circuits and Systems I Communications and Computer Sciences*, vol. 41, no. 6, June 1994.
- [15] G. H. Yuan, S. Banerjee, E. Ott, and J. A. Yorke, “Border collision bifurcations in the buck converter,” *IEEE Transactions on Circuits and Systems-I*, vol. 45, no. 7, pp. 707–716, 1998.
- [16] S. Banerjee, P. Ranjan, and C. Grebogi, “Bifurcations in two-dimensional piecewise smooth maps — theory and applications in switching circuits,” *IEEE Transactions on Circuits and Systems-I*, vol. 47, no. 5, pp. 633–643, 2000.
- [17] R.I. Leine, D.H. Van Campen, and B.L. Van de Vrande, “Bifurcations in nonlinear discontinuous systems,” *Nonlinear Dynamics*, vol. 23, pp. 105–164, 2000.
- [18] R.I. Leine and D.H. Van Campen, “Discontinuous fold bifurcations in mechanical systems,” *Archive of Applied Mechanics*, vol. 72, pp. 138–146, 2002.
- [19] A.B. Nordmark, “Non-periodic motion caused by grazing incidence in impact oscillators,” *Journal of Sound and Vibration*, vol. 2, pp. 279–297, 1991.
- [20] M.H. Frederiksson and A.B. Nordmark, “Bifuractions caused by grazing incidence in many degrees of freedom impact oscillators,” *Proc. Royal Soc. Lond. A*, vol. 453, pp. 1261–1276, June 1997.
- [21] A.B. Nordmark, “Universal limit mapping in grazing bifurcations,” *Physical Review E*, vol. 55, pp. 266–270, 1997.
- [22] H. Dankowicz and A.B. Nordmark, “On the origin and bifurcations of stick-slip oscillations,” *Physica D*, vol. 136, no. 3-4, pp. 280–302, Feb 2000.
- [23] V. Firoiu and M. Borden, “A study of active queue management for congestion control,” *Proceedings of Infocom*, 2000.
- [24] C.H. Hommes and H.E. Nusse, “Period 3 to period 2 bifurcation for piecewise linear-models,” *Journal of Economics*, vol. 54, no. 2, pp. 157–169, 1991.
- [25] J. Sun et al., “Alternans and period-doubling bifurcations in atrioventricular nodal conduction,” *Journal Theoretical Biology*, vol. 173, pp. 79–91, 1995.
- [26] J. Alvarez-Ramirez, “Dynamics of controlled-linear discrete time systems with a dead-zone nonlinearity,” in *American Control Conference*, 1994, vol. 1, pp. 761–765.
- [27] M. di Bernardo, “Controlling switching systems: a bifurcation approach,” *IEEE International Symposium on Circuits and Systems*, vol. 2, pp. 377–380, 2000.

- [28] M. di Bernardo and G. Chen, “Controlling bifurcations in nonsmooth dynamical systems,” in *Controlling Chaos and Bifurcations in Engineering Systems*, G. Chen and X. Dong, Eds., chapter 18, pp. 391–412. CRC Press, Boca Raton, FL, 2000.
- [29] S. Parui and S. Banerjee, “Border collision bifurcations at the change of state-space dimension,” Submitted.
- [30] K.T. Alligood, T.D. Sauer, and J.A. Yorke, *Chaos: An Introduction to Dynamical Systems*, Springer-Verlag, New York, 1996.
- [31] D.P. Lindorff, *Theory of Sampled-Data Control Systems*, Wiley, New York, 1965.
- [32] T. Kailath, *Linear Systems*, Prentice-Hall, Englewood Cliffs, NJ, 1980.
- [33] D.J. Christini and J.J. Collins, “Using chaos control and tracking to suppress a pathological nonchaotic rhythms in cardiac model,” *Physical Review E*, vol. 53, no. 1, pp. R49–R51, Jan 1996.
- [34] M.E. Brandt, H.T. Shih, and G. Chen, “Linear time-dely feedback control of a pathological rhythm in a cardiac conduction model,” *Physical Review E*, vol. 56, no. 2, pp. R1334–R1337, Aug 1997.
- [35] K. Hall et al., “Dynamic control of cardiac alternans,” *Physical Review Letters*, vol. 78, pp. 4518–4521, 1997.
- [36] D. Chen, H.O. Wang, and W. Chin, “Suppressing cardiac alternans: Analysis and control of a border-collision bifurcation in a cardiac conduction model,” in *IEEE International Symposium on Circuits and Systems*, 1998, vol. 3, pp. 635–638.